

## Supporting Information

### **Carborane photochromism: A fatigue resistant carborane switch**

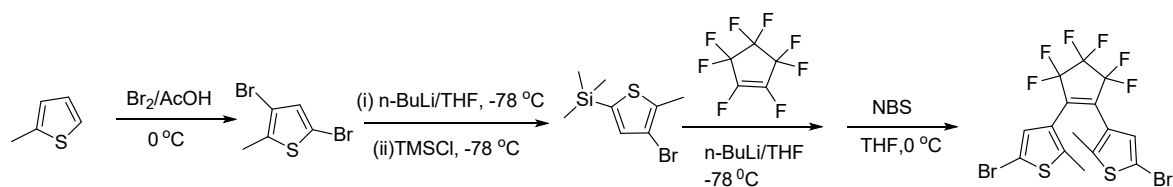
*Chong Li,\* Matthew P. Aldred, Rachel A. Harder, Chen Ying, Dmitry S. Yufit, Ming-Qiang Zhu and Mark A. Fox\**

#### *List of Contents*

General Experimental Details	S2
Computations	S6
Syntheses and Characterisation	S7
NMR Spectra	S12
Mass Spectra	S19
IR Spectra	S20
Photophysics	S21
Cyclic Voltammetry	S30
X-ray Crystallography	S33
Optimised Geometries	S36
Simulated Absorption Spectra	S39
References	S42

## General Experimental Details

All commercially available chemicals were used without further purification unless stated otherwise. 1,2-bis[2-bromo-5-methyl-3-thienyl]perfluorocyclopentene (**Scheme S1**) was synthesised as reported in the literature.<sup>1</sup> Reactions requiring an inert atmosphere were performed under a blanket of argon gas which was dried over a phosphorus pentoxide column. Anhydrous solvents were dried through an HPLC column on an Innovative Technology Inc. solvent purification system. Column chromatography was performed using 40-60  $\mu\text{m}$  mesh silica gel. Analytical TLC was performed on plates pre-coated with silica gel (Merck, silica gel 60F<sub>254</sub>) and visualised using UV light (254, 315, 365 nm). NMR spectra were recorded on Bruker Avance 400 MHz, Varian Mercury 200 and 400 MHz, Varian Inova 500 MHz or Varian VNMRS 600 and 700 MHz spectrometers. 2D <sup>1</sup>H–<sup>1</sup>H COSY and <sup>1</sup>H–<sup>13</sup>C correlation (HSQC and HMBC) NMR spectra were recorded on the VNMRS-700 spectrometer. <sup>1</sup>H and <sup>13</sup>C chemical shifts are referenced to tetramethylsilane [TMS, Si(CH<sub>3</sub>)<sub>4</sub>] at 0.00 ppm (internal <sup>1</sup>H reference for residual CHCl<sub>3</sub> in CDCl<sub>3</sub> at 7.28 ppm and internal <sup>13</sup>C reference for CDCl<sub>3</sub> at 77.0 ppm), <sup>19</sup>F chemical shifts are referenced externally to CFCl<sub>3</sub> at 0.0 ppm and <sup>11</sup>B chemical shifts are referenced externally to BF<sub>3</sub>·Et<sub>2</sub>O at 0.0 ppm. The expected very weak multiplets for CF<sub>2</sub> in the <sup>13</sup>C{<sup>1</sup>H} spectra for compounds **1** and **2** were not observed. Neat IR spectra were measured on a Perkin Elmer 1600 series FTIR with an ATR probe. ASAP mass spectra were recorded on a Waters Xevo QTOF spectrometer. Elemental analyses were obtained on an Exeter Analytical Inc. CE-440 elemental analyser. Where solvent mixtures are mentioned any percentage/ratio is by volume.



**Scheme S1.** Steps carried out to synthesise the precursor 1,2-bis[2-bromo-5-methyl-3-thienyl]perfluorocyclopentene.<sup>1</sup>

## Electrochemistry

Cyclic voltammetry (CV) measurements were recorded at a scan rate of 100 mV s<sup>-1</sup> at room temperature using an air-tight single-compartment three-electrode cell equipped with a Pt working electrode (1.2 mm surface diameter), Pt wire counter electrode and Pt wire pseudo-reference electrode. The cell was connected to a computer-controlled Autolab PG-STAT 30 potentiostat using GPES software. The solutions contained the compound (1 mg/mL) and *n*-Bu<sub>4</sub>NPF<sub>6</sub> (0.1 M) as the supporting electrolyte in dichloromethane (DCM). The decamethylferrocenium /decamethylferrocene internal reference couple (C<sub>5</sub>Me<sub>5</sub>)<sub>2</sub>Fe<sup>+</sup> / (C<sub>5</sub>Me<sub>5</sub>)<sub>2</sub>Fe = (Cp\*Fe<sup>+</sup>/Cp\*Fe) at -0.53 V is referenced against the ferrocenium/ferrocene reference couple at 0.00 V.

## Photophysical measurements

Solution-state measurements were carried out in quartz cuvettes with a path length of 1 cm. Solid state measurements were obtained from powder forms. Absorbance spectra were measured on a Cary 5000 UV-Vis-NIR spectrometer with Cary WinUV Scan software. Emission spectra were recorded on a Jobin Yvon Fluorolog-3 luminescence spectrometer with a CCD detector using FluorEssence software. The photoluminescence quantum yield (PLQY) for **2** as powder was measured using a calibrated Quanta-φ integrating sphere coupled with a Jobin Yvon FluoroLog-3 spectrometer and PMT detector (0.5 s integration time) and analysed using FluorEssence software. Time-resolved measurements (TCSPC, time-correlated single-photon counting) were performed on a Horiba Deltaflex system with EzTime software.

PMMA films were prepared by spin coating of chloroform solutions containing PMMA polymer (100 mg/mL) and carborane DTE photoswitches (2 mg/mL) at 900 rpm for 10 s and then 3000 rpm for 60 s onto clean quartz plates. The carborane DTE photoswitch **2** was dissolved in THF to make a stock solution with concentrations of  $1.0 \times 10^{-3}$  mol/L for preparation of water/THF solutions. The solutions were then diluted with pure THF 5 times to obtain a solution with concentrations of  $2.0 \times 10^{-4}$  mol/L. Injecting 30  $\mu$ L of the above as-prepared solutions into 3 mL solvents (such as THF, water, THF/water binary solvent), the solutions with the concentration of  $2.0 \times 10^{-6}$  mol/L were obtained and used for the optical tests. The photoluminescence quantum yield (PLQY) for **2** in THF was measured using an Edinburgh FLSP920 spectrometer with quinine sulfate in 0.1 M H<sub>2</sub>SO<sub>4</sub> (PLQY = 0.54) as reference.

### **Photoisomerisation measurements**

The carborane DTE photoswitches solutions of toluene ( $2.0 \times 10^{-6}$  M) was placed in 1 cm cuvette for photoisomerisation quantum yield measurements. The UV-vis spectrum was recorded using a Shimadzu UV-vis-NIR Spectrophotometer (UV-3600). The PL spectrum was recorded using Edinburgh instruments (FLSP920 spectrometers). The 302 nm UV light was used by an ultraviolet transmission platform (with 4 ultraviolet tubes, each 8W 220 V, the measured power is 0.96 mW/cm<sup>2</sup>) and the visible light was used by a 621 nm LED that the measured power is 7.68 mW/cm<sup>2</sup>.

The quantum yields of photoisomerisation reactions were measured following the reported method (Equation S1-S7).<sup>2-4</sup> The kinetic process of re-equilibration from an arbitrary initial photostationary state ( $A_0$ ) to a new photostationary state ( $A_{\text{pss}}$ ), dictated by exposure to light of a given wavelength, is monoexponential. The rate constant of equilibration ( $\kappa_{\text{eq}}$ ) is given by the sum of the two apparent first-order rate constants defining the overall transition and the equilibrium constant ( $K_{\text{pss}}$ ) by their ratio.  $\kappa_{\text{ex}}$  is the rate constant for absorption at excitation wavelength.  $\sigma_{\text{ex}}$  (cm<sup>2</sup> molecule<sup>-1</sup>) is the absorption cross-section at excitation

wavelength  $\lambda_{\text{irr}}$  (nm).  $\psi_{\text{ex}}$  (photons  $\text{s}^{-1}\text{cm}^{-2}$ ) is the photon flux.  $I$  ( $\text{W cm}^{-2}$ ) is the intensity of irradiation light (302 nm and 621 nm).  $N_{\text{a}}$  is the Avogadro's constant. Concentration in toluene =  $2.0 \times 10^{-6}$  M.

$$A(t) = A_{\text{pss}} + (A_0 - A_{\text{pss}}) e^{-\kappa_{\text{eq}} t} \quad (\text{Equation S1})$$

$$\kappa_{\text{eq}} = \kappa_{\text{o} \rightarrow \text{c}} + \kappa_{\text{c} \rightarrow \text{o}}, \quad (\text{Equation S2})$$

$$K_{\text{pss}} = [\text{open form}] / [\text{closed form}] = \kappa_{\text{o} \rightarrow \text{c}} / \kappa_{\text{c} \rightarrow \text{o}} \quad (\text{Equation S3})$$

$$\alpha_{\text{pss}} = K_{\text{pss}} / (1 + K_{\text{pss}}) = \kappa_{\text{o} \rightarrow \text{c}} / \kappa_{\text{eq}} \quad (\text{Equation S4})$$

$$\kappa_{\text{ex}} = \sigma_{\text{ex}} \psi_{\text{ex}}, \quad \sigma_{\text{ex}} = (10^3 \ln 10 / N_{\text{a}}) \epsilon_{\text{irr}}, \quad \psi_{\text{ex}} = 5 \times 10^{15} \lambda_{\text{irr}} I \quad (\text{Equation S5})$$

$$\Phi_{\text{o} \rightarrow \text{c}} = \kappa_{\text{o} \rightarrow \text{c}} / \kappa_{\text{ex, o}} \quad (\text{Equation S6})$$

$$\Phi_{\text{c} \rightarrow \text{o}} = \kappa_{\text{c} \rightarrow \text{o}} / \kappa_{\text{ex, c}} \quad (\text{Equation S7})$$

$\lambda_{\text{irr}}$  is the irradiation wavelength for photoisomerisation, the intensity of irradiation light is 0.591 or 1.832  $\text{mW}/\text{cm}^2$  for 302 nm and 7.684  $\text{mW}/\text{cm}^2$  for 621 nm.

$\epsilon_{\text{irr}}$  is the molar extinction coefficient at wavelength  $\lambda_{\text{irr}}$ .

$\alpha_{\text{pss}}$  is the fractional population of closed form in PSS irradiated under given wavelengths (obtained from the  $^1\text{H}$  NMR data, Figure S28).

$\kappa_{\text{eq}}$  is the rate constant of equilibration, which was fit with a monoexponential curve from the kinetics of re-equilibration from an arbitrary initial photostationary state ( $\alpha_{\text{o}}$ ) to a new photostationary state ( $\alpha_{\text{pss}}$ ).

$\kappa_{\text{ex}}$  is the excitation rate constant.

$\Phi$  is the cyclisation ( $\text{o} \rightarrow \text{c}$ ) or cycloreversion ( $\text{c} \rightarrow \text{o}$ ) quantum yield.

## Single-crystal X-ray Crystallography

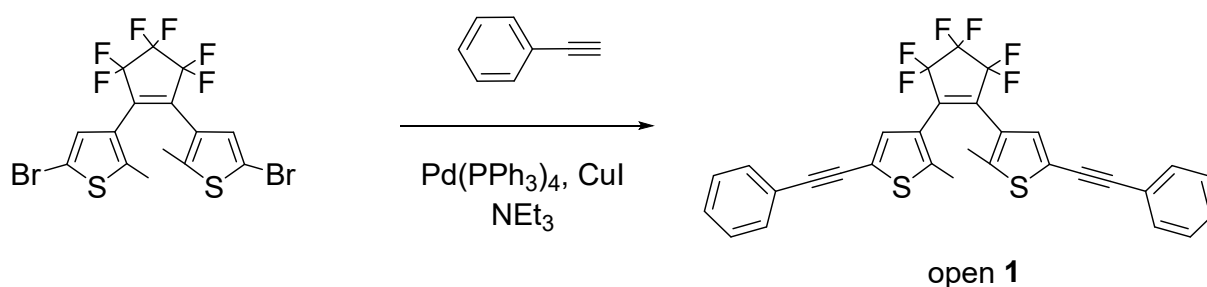
The X-ray single crystal data were collected on a Bruker D8Venture (compound **2**; Photon100 CMOS detector, I $\mu$ S-microsource, focusing mirrors) and Agilent XCalibur (compound **1**, Sapphire-3 CCD detector, fine-focus sealed tube, graphite monochromator) diffractometers equipped with Cryostream (Oxford Cryosystems) open-flow nitrogen cryostats at temperature 120.0(2) K. The data for compound **2** were collected using  $\lambda$ MoK $\alpha$  radiation ( $\lambda = 0.71073 \text{ \AA}$ ). All structures were solved by direct method and refined by full-matrix least squares on F<sup>2</sup> for all data using Olex2<sup>5</sup> and SHELXTL<sup>6</sup> software. All non-disordered non-hydrogen atoms were refined anisotropically, the hydrogen atoms were placed in the calculated positions and refined in riding mode. Atoms of disordered groups (CF<sub>2</sub> groups in structures **1** and **2**, toluene molecule in structure **2**) were refined in isotropic approximation with fixed SOFs. Crystal data and parameters of refinement are listed in Table S7. Crystallographic data for the structure have been deposited with the Cambridge Crystallographic Data Centre as supplementary publication CCDC-2070456-2070457.

## Computations

Geometry optimisations were carried out with the Gaussian 16 package.<sup>7</sup> Ground state (S<sub>0</sub>) geometries were fully optimised from different starting geometries without symmetry constraints at the hybrid-DFT functional B3LYP<sup>8,9</sup> with the 6-31(d) basis set<sup>10,11</sup> and the Grimme dispersion factor, GD3BJ.<sup>12</sup> Electronic structure calculations on the optimised geometries provided the frontier orbitals and their energies. The predicted absorption spectra were produced visually from 60 lowest singlet states determined by time dependent-density functional theory (TD-DFT). Natural transition orbital (NTO) calculations were performed at TD-DFT on the optimised S<sub>0</sub> geometries to visualise the various transitions. The molecular orbital (MO) and NTO figures were generated using the Gabedit package.<sup>13</sup>

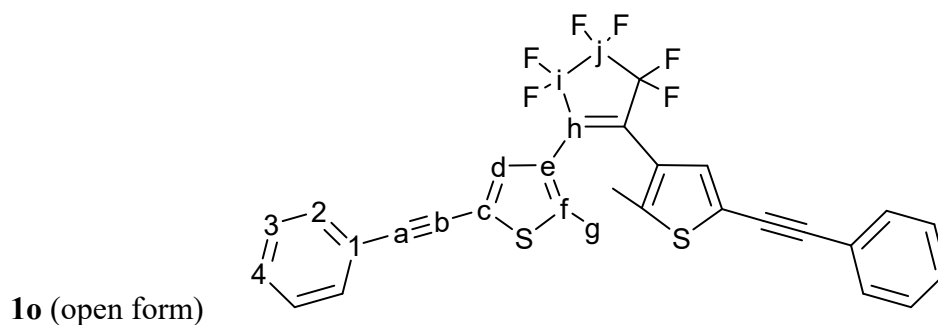
## Syntheses and Characterisation data for **1** and **2**

### *1,2-Bis(5-phenylethynyl-2-methyl-3-thienyl)-perfluorocyclopentene 1*

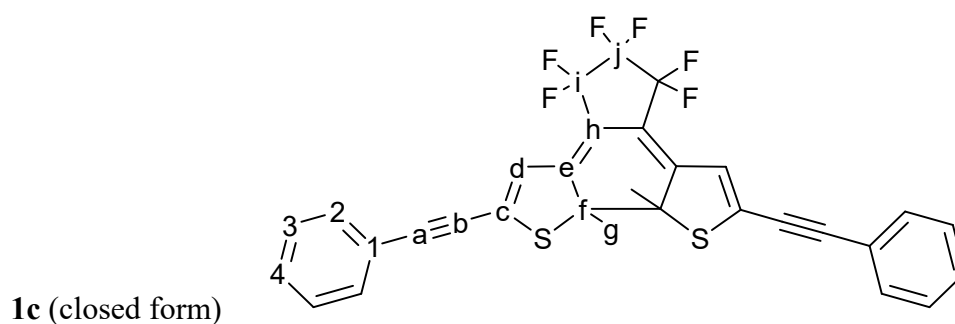


To a 100-mL round-bottom flask, 1,2-bis[2-bromo-5-methyl-3-thienyl]perfluorocyclopentene (3.14 g, 6 mmol),  $\text{Pd}(\text{PPh}_3)_4$  (0.35 g, 0.60 mmol),  $\text{CuI}$  (0.057 g, 0.30 mmol), phenylacetylene (1.3 g, 13 mmol) and anhydrous triethylamine (50 mL) was added under  $\text{N}_2$  atmosphere. The reaction mixture was heated at 50 °C for 24 h. Solvent and excess aryl alkyne were removed in vacuo. The mixture was extracted with diethyl ether followed by washing with water for 3 times, and the organic layer was washed with water (150 mL  $\times$  3), dried over  $\text{Na}_2\text{SO}_4$ , and concentrated under reduced pressure. The crude product was purified by gravity silica-gel column chromatography and eluted with hexane to yield a light blue solid **1** (2.91 g, 85%). Crystals suitable for X-ray structural determination were grown from chloroform. Compound **1** has been reported elsewhere<sup>14</sup> but no synthetic details given.

IR (neat solid):  $\nu = 3053$  (w;  $\nu(\text{aromatic C-H})$ ), 2909 (w;  $\nu(\text{alkyl C-H})$ ), 2213 (w;  $\nu(\text{alkynyl C-C})$ ), 1633 (w;  $\nu(\text{cyclopentenyl C=C})$ ), 1596 (m;  $\nu(\text{aromatic C-C})$ ), 1493 (m), 1339 (m), 1272 (s), 1259 (s), 1186 (m), 1139 (s), 1117 (s), 1099 (s), 1084 (m), 1042 (s), 984 (m), 751 (s), 738 (s), 688 (s), 517 (s)  $\text{cm}^{-1}$  (s); UV-vis (tetrahydrofuran (THF),  $2 \times 10^{-5}$  M):  $\lambda_{\text{max}}(\epsilon) = 306$  (55000) open form, 606 (20000) closed form (PSS); ASAP  $m/z$  (%): 569 (100) [ $\text{M}^+ + \text{H}$ ], [568 (16) [ $\text{M}^+$ ]; calcd for  $\text{C}_{31}\text{H}_{18}\text{F}_6\text{S}_2$ , 568. Anal. calcd for  $\text{C}_{31}\text{H}_{18}\text{F}_6\text{S}_2$ : C 65.48, H 3.19; found: C 65.37, H 3.13.

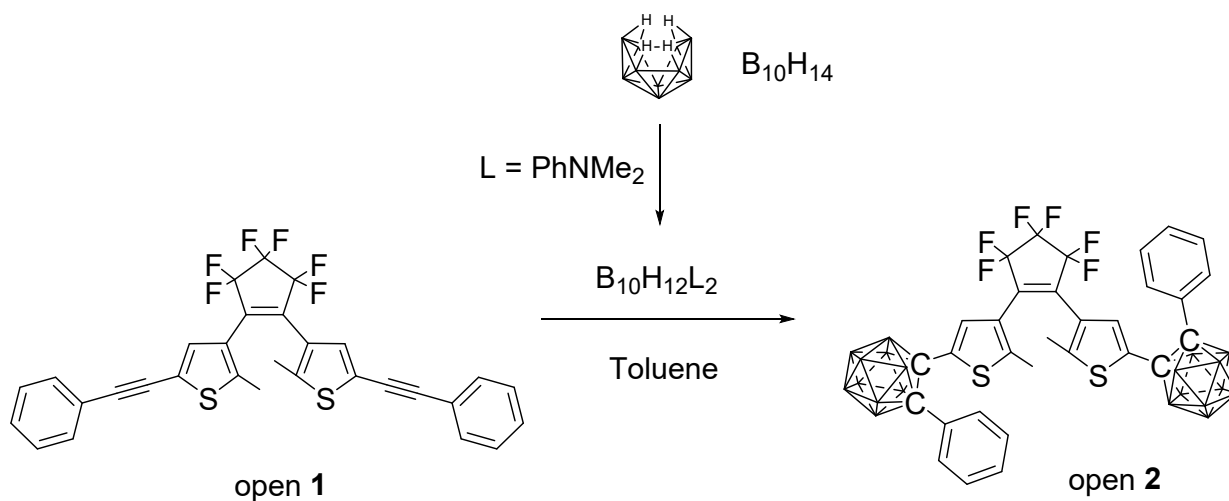


$^1\text{H}$  (400 MHz,  $\text{CDCl}_3$ ,  $\delta$ ): **1o** (open form): 7.54 (m, 4H; H2), 7.39 (m, 6H; H3 + H4), 7.29 (s, 2H; Hd), 1.98 (s, 6H; Hg);  $^{19}\text{F}\{^1\text{H}\}$  NMR (376 MHz,  $\text{CDCl}_3$ ,  $\delta$ ): **1o**: -110.3 (t,  $^3J_{\text{FF}} = 5.5$  Hz, 4F; Fi), -131.8 (quintet,  $^3J_{\text{FF}} = 5.5$  Hz, 2F; Fj);  $^{13}\text{C}\{^1\text{H}\}$  NMR (100 MHz,  $\text{CDCl}_3$ ,  $\delta$ ): **1o**: 143.4 (Cf), 136.1 (Ch), 131.5 (C2), 131.3 (Cd), 128.8 (C4), 128.5 (C3), 124.8 (Ce), 122.4 (C1), 121.9 (Cc), 94.0 (Ca), 81.5 (Cb), 14.5 (Cg).

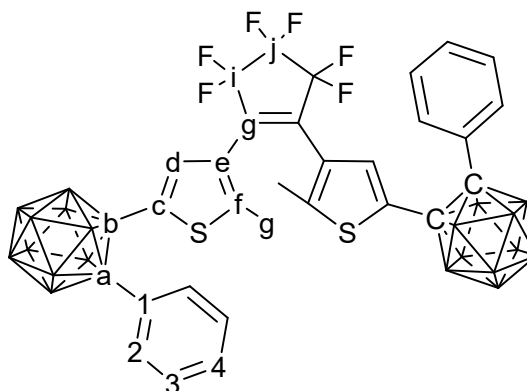


$^1\text{H}$  (400 MHz,  $\text{CDCl}_3$ ,  $\delta$ ): **1c** (closed form): 7.53 (dd,  $^3J_{\text{HH}} = 7$  Hz, 4H; H2), 7.42 (m, 6H; H3 + H4), 6.51 (s, 2H; Hd), 2.23 (s, 6H; Hg);  $^{19}\text{F}\{^1\text{H}\}$  NMR (376 MHz,  $\text{CDCl}_3$ ,  $\delta$ ): **1c**: -112.3 (dq,  $^2J_{\text{FF}} = 256$  Hz,  $^3J_{\text{FF}} = 6$  Hz,  $^5J_{\text{FF}} = 6$  Hz, 2F; Fi), -114.1 (dq,  $^2J_{\text{FF}} = 256$  Hz,  $^3J_{\text{FF}} = 6$  Hz,  $^5J_{\text{FF}} = 6$  Hz, 2F; Fj), -133.4 (quintet,  $^3J_{\text{FF}} = 6$  Hz, 2F; Fj);  $^{13}\text{C}\{^1\text{H}\}$  NMR (100 MHz,  $\text{CDCl}_3$ ,  $\delta$ ): **1c**: 148.9 (Ce), 137.3 (Cc), 131.9 (C2), 129.9 (C4), 128.6 (C3), 123.4 (Cd), 121.4 (C1), 118.0 (Ch), 103.5 (Ca), 83.6 (Cb), 66.9 (Cf), 25.2 (Cg).

*1,2-Bis{5-[1'-(2'-phenyl-1',2'-dicarbadodecaboranyl)]-2-methyl-3-thienyl}-perfluorocyclopentene 2*

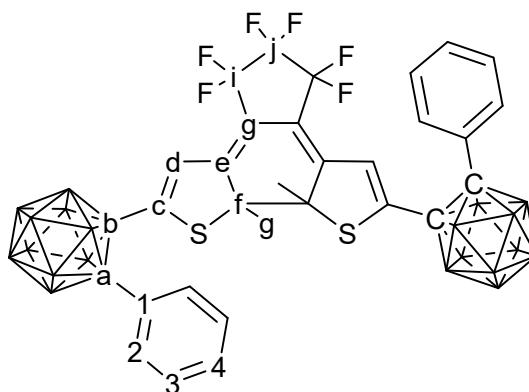


Decaborane ( $\text{B}_{10}\text{H}_{14}$ ) (0.63 g, 5.2 mmol) and *N,N*-dimethylaniline (1.3 g, 10.7 mmol) in 20 mL of distilled toluene was stirred for 10 min under an Ar atmosphere. The temperature was then raised to 80 °C for 2 h. After cooling to 30 °C when the mixture became cloudy, 1,2-bis(5-phenylethynyl-2-methyl-3-thienyl)-perfluorocyclopentene **1** (1.47 g, 2.6 mmol) was added in one portion and the final mixture was refluxed for 2 h. Hexane (10 mL) was added, the resulting solid was filtered and dried under vacuo. The residue was purified using silica gel column chromatography with chloroform as the eluent to yield a white solid **2** (1.16 g, 56%). Crystals suitable for X-ray structural determination were grown from toluene. **2** IR (neat solid):  $\nu = 3064$  (w;  $\nu(\text{aromatic C-H})$ ), 2962 (w;  $\nu(\text{alkyl C-H})$ ), 2600 (s;  $\nu(\text{carborane B-H})$ ), 2588 (s;  $\nu(\text{carborane B-H})$ ), 2560 (s;  $\nu(\text{carborane B-H})$ ), 1446 (m), 1330 (m), 1269 (s), 1195 (s), 1125 (s), 1117 (s), 1090 (m), 1070 (m), 1062 (m), 1045 (m), 754 (m), 727 (m), 690 (s), 525 (m), 484  $\text{cm}^{-1}$  (m); UV-vis (THF,  $2 \times 10^{-5}$  M):  $\lambda_{\text{max}}(\epsilon) = 562$  (90000) closed form (PSS); ASAP  $m/z$  (%): 805 (100) [ $\text{M}^+ - 3\text{H}$ ], [808 (43) [ $\text{M}^+$ ]]; calcd for  $\text{C}_{31}\text{H}_{38}\text{B}_{20}\text{F}_6\text{S}_2$ , 808. Anal. calcd for  $\text{C}_{31}\text{H}_{38}\text{B}_{20}\text{F}_6\text{S}_2$ : C 46.26, H 4.76; found: C 46.02, H 4.76.



**2o** (open form)

$^1\text{H}\{^{11}\text{B}\}$  (400 MHz,  $\text{CDCl}_3$ ,  $\delta$ ): **2o**: 7.54 (d,  $^3J_{\text{HH}} = 7$  Hz, 4H; H2), 7.37 (t,  $^3J_{\text{HH}} = 7$  Hz, 2H; H4), 7.26 (t,  $^3J_{\text{HH}} = 7$  Hz, 4H; H3), 6.89 (s, 2H; Hd), 3.09 (s, 4H; BH), 2.53 (s, 12H; BH), 2.34 (s, 4H; BH), 1.26 (s, 6H; Hg);  $^{19}\text{F}\{^1\text{H}\}$  NMR (376 MHz,  $\text{CDCl}_3$ ,  $\delta$ ): **2o**: -110.4 (t,  $^3J_{\text{FF}} = 5$  Hz, 4F; Fi), -131.9 (quintet,  $^3J_{\text{FF}} = 5$  Hz, 2F; Fj);  $^{11}\text{B}\{^1\text{H}\}$  NMR (128 MHz,  $\text{CDCl}_3$ ,  $\delta$ ): **2o**: -2.2 (4B), -8.8 (4B), -10.3 (12B);  $^{13}\text{C}\{^1\text{H}\}$  NMR (100 MHz,  $\text{CDCl}_3$ ,  $\delta$ ): **2o**: 145.1 (Cf), 135.3 (Ch), 133.2 (Cc), 131.1 (C2), 130.9 (Cd), 130.6 (C4), 130.4 (C1), 128.6 (C3), 124.4 (Ce), 85.9 (Ca), 78.8 (Cb), 14.0 (Cg).



**2c** (closed form)

$^1\text{H}\{^{11}\text{B}\}$  (400 MHz,  $\text{CDCl}_3$ ,  $\delta$ ): **2c**: 7.62 (d,  $^3J_{\text{HH}} = 7$  Hz, 4H; H2), 7.45 (t,  $^3J_{\text{HH}} = 7$  Hz, 2H; H4), 7.37 (t,  $^3J_{\text{HH}} = 7$  Hz, 4H; H3), 6.12 (s, 2H; Hd), 3.01 (s, 2H; BH), 2.96 (s, 2H; BH), 2.58 (s, 4H; BH), 2.49 (s, 8H; BH), 2.35 (s, 4H; BH), 1.33 (s, 6H; Hg);  $^{19}\text{F}\{^1\text{H}\}$  NMR (376 MHz,  $\text{CDCl}_3$ ,  $\delta$ ): **2c**: -112.7 (dq,  $^2J_{\text{FF}} = 259$  Hz,  $^3J_{\text{FF}} = 5.5$  Hz,  $^5J_{\text{FF}} = 5.5$  Hz, 2F; Fi), -114.6 (dq,  $^2J_{\text{FF}} = 259$  Hz,  $^3J_{\text{FF}} = 5.5$  Hz,  $^5J_{\text{FF}} = 5.5$  Hz, 2F; Fi), -133.8 (quintet,  $^3J_{\text{FF}} = 5.5$  Hz, 2F; Fj);  $^{11}\text{B}\{^1\text{H}\}$

NMR (128 MHz, CDCl<sub>3</sub>, δ): **2c**: -2.6 (4B), -10.0 (16B); <sup>13</sup>C{<sup>1</sup>H} NMR (100 MHz, CDCl<sub>3</sub>, δ):  
**2c**: 150.7 (Cc), 148.3 (Ce), 131.2 (C2), 131.0 (C4), 129.9 (C1), 128.7 (C3), 123.0 (Cd), 119.7  
(Ch), 85.5 (Ca), 77.6 (Cb), 66.3 (Cf), 23.7 (Cg).

## NMR Spectra for 1 and 2

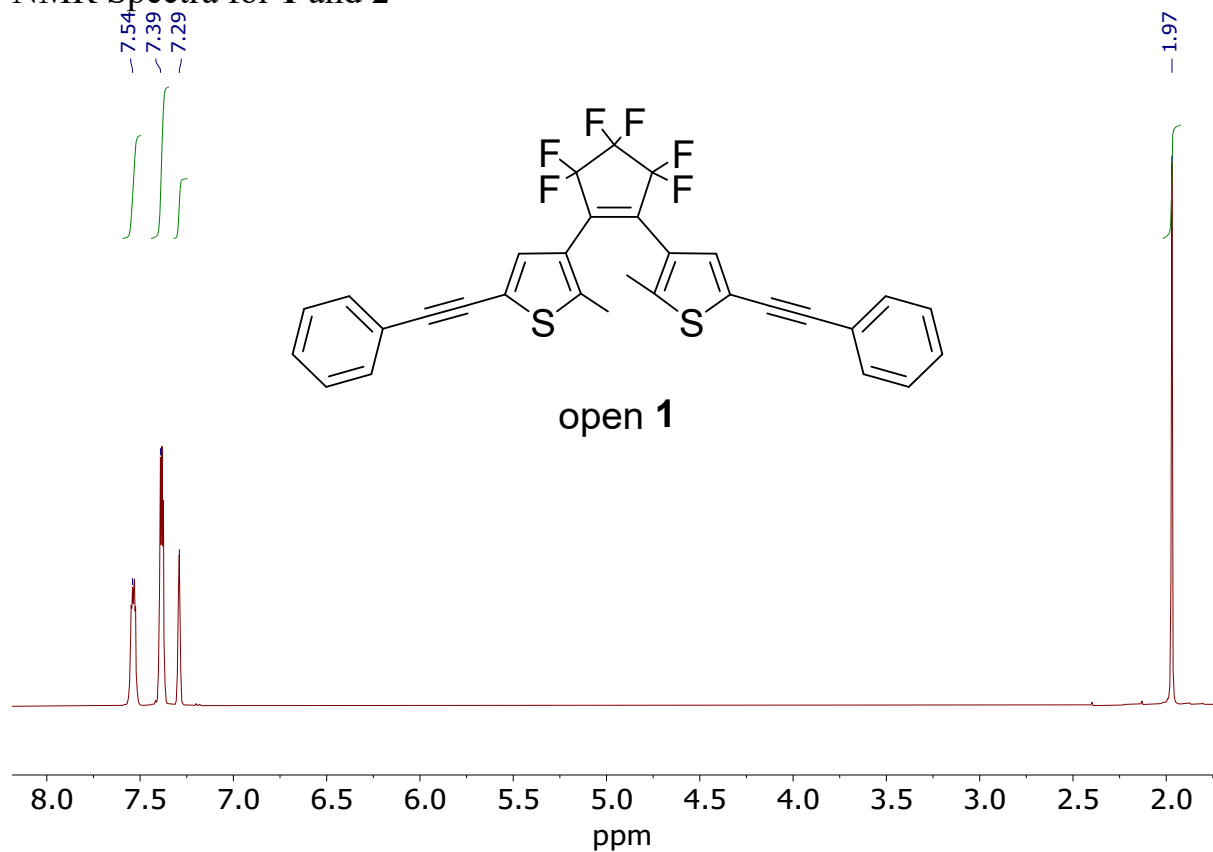


**Figure S1.** <sup>1</sup>H NMR spectrum for open 1.

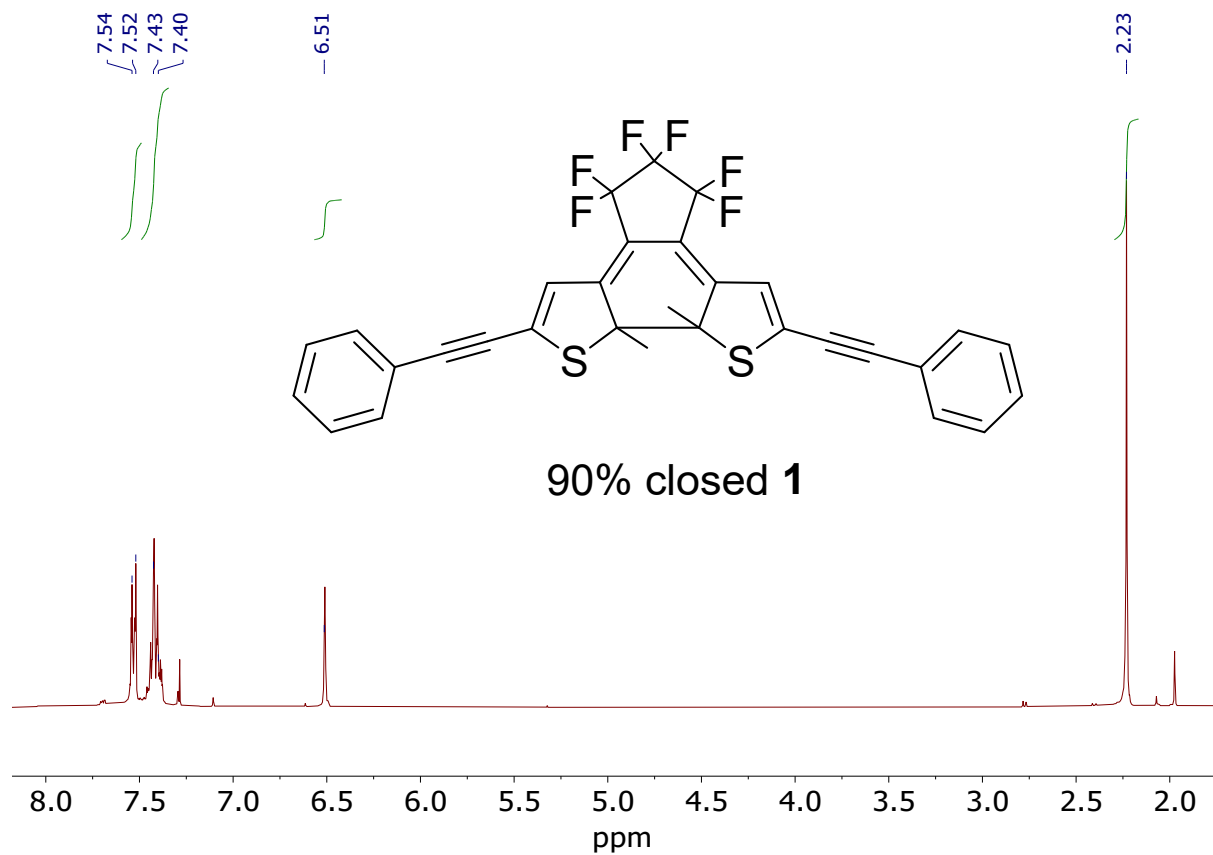


**Figure S2.** <sup>1</sup>H NMR spectrum for closed 1.



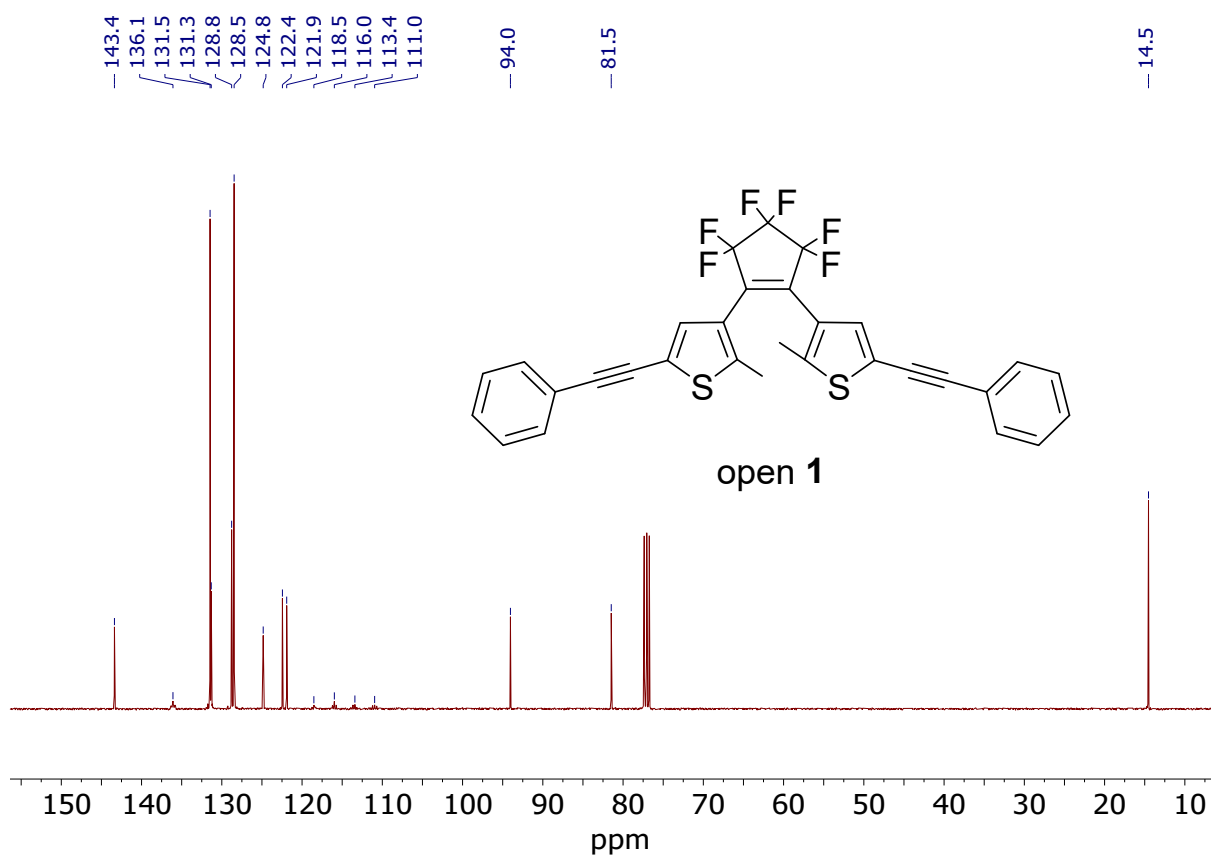


**Figure S5.**  $^{13}\text{C}\{^1\text{H}\}$  NMR spectrum for **open 1**.

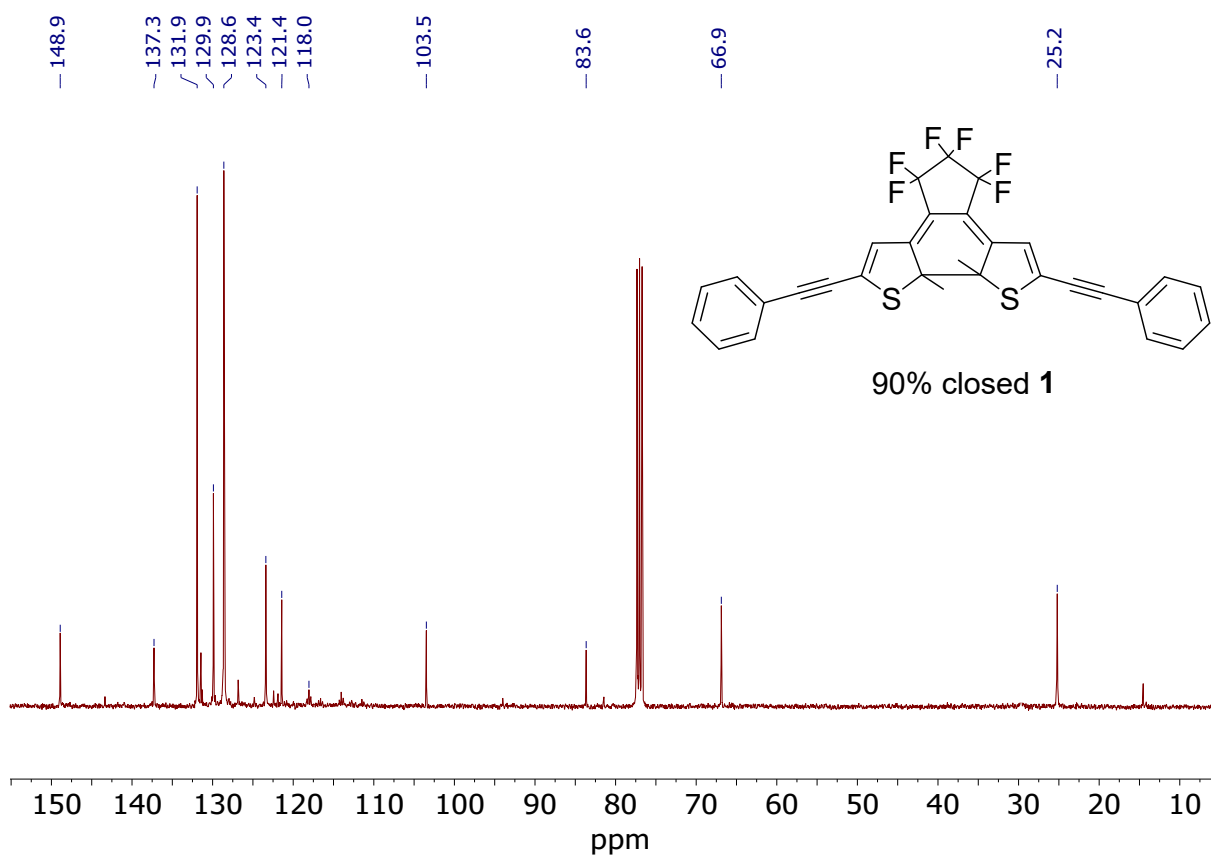


**Figure S6.**  $^{13}\text{C}\{^1\text{H}\}$  NMR spectrum for **closed 1**.

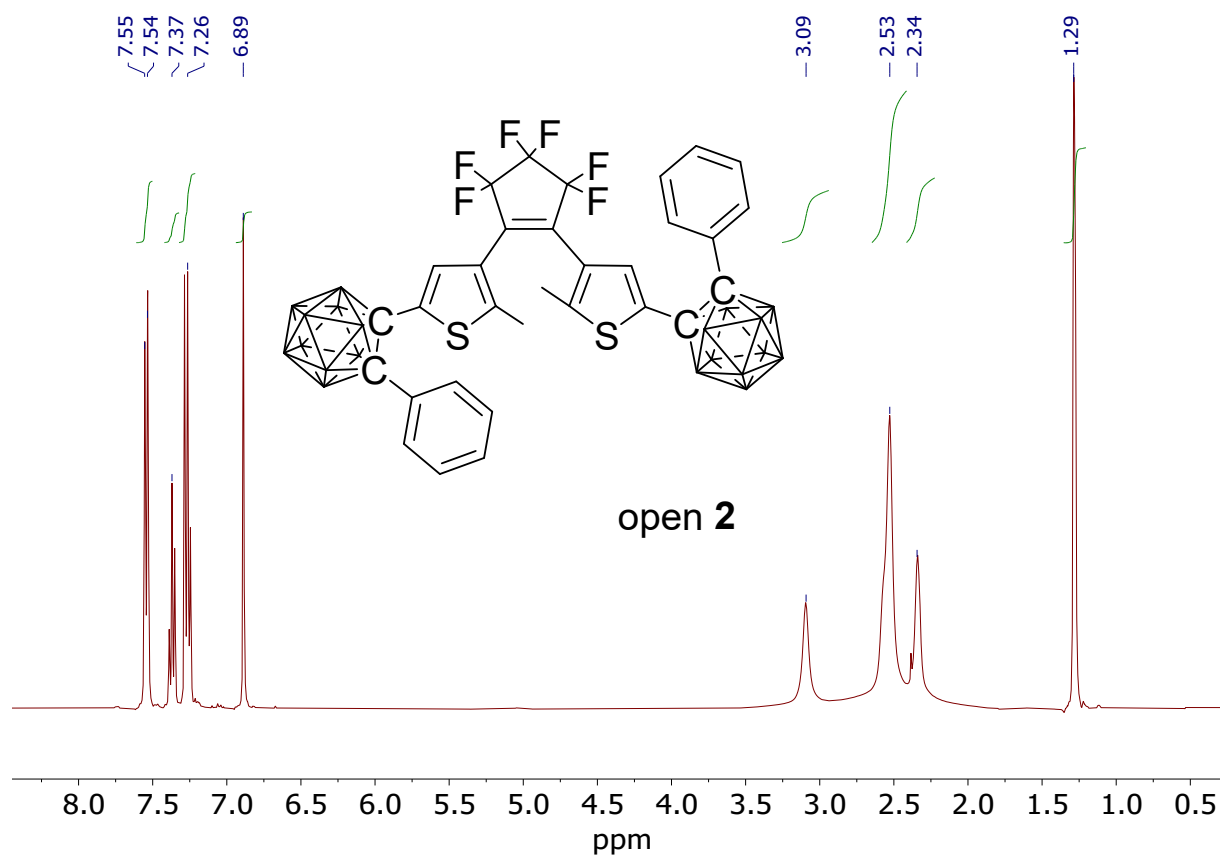


**Figure S7.**  $^1\text{H}\{^{11}\text{B}\}$  NMR spectrum for **open 2**.

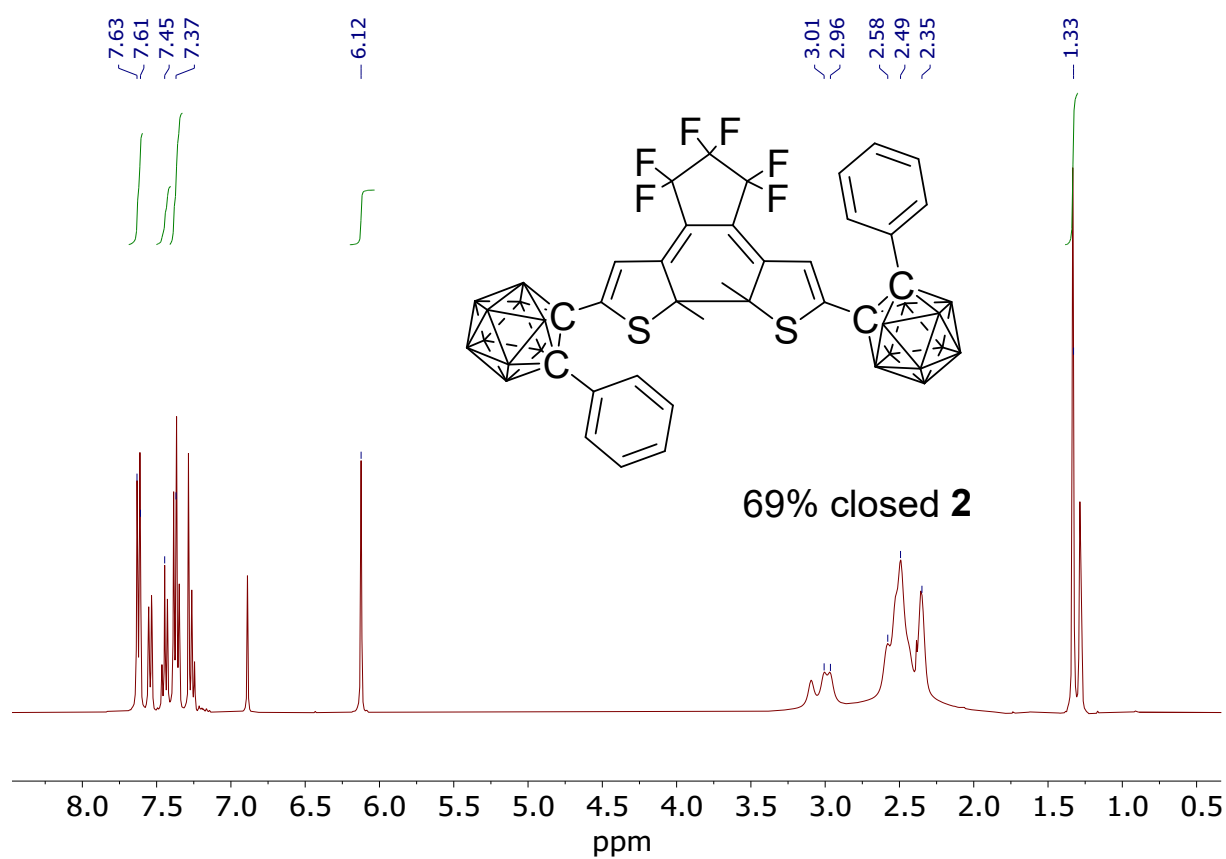


**Figure S8.**  $^1\text{H}\{^{11}\text{B}\}$  NMR spectrum for **closed 2**.



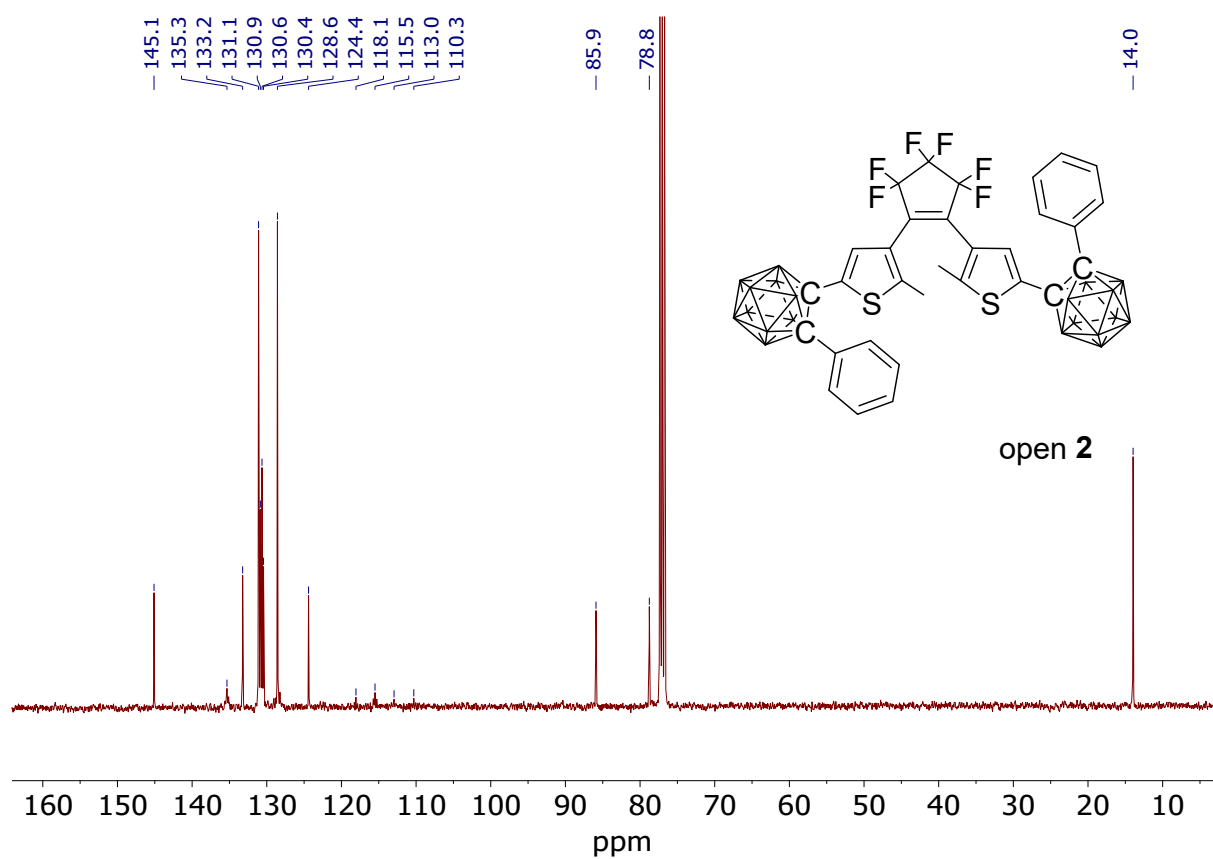


**Figure S11.**  $^{13}\text{C}\{^1\text{H}\}$  NMR spectrum for open **2**.

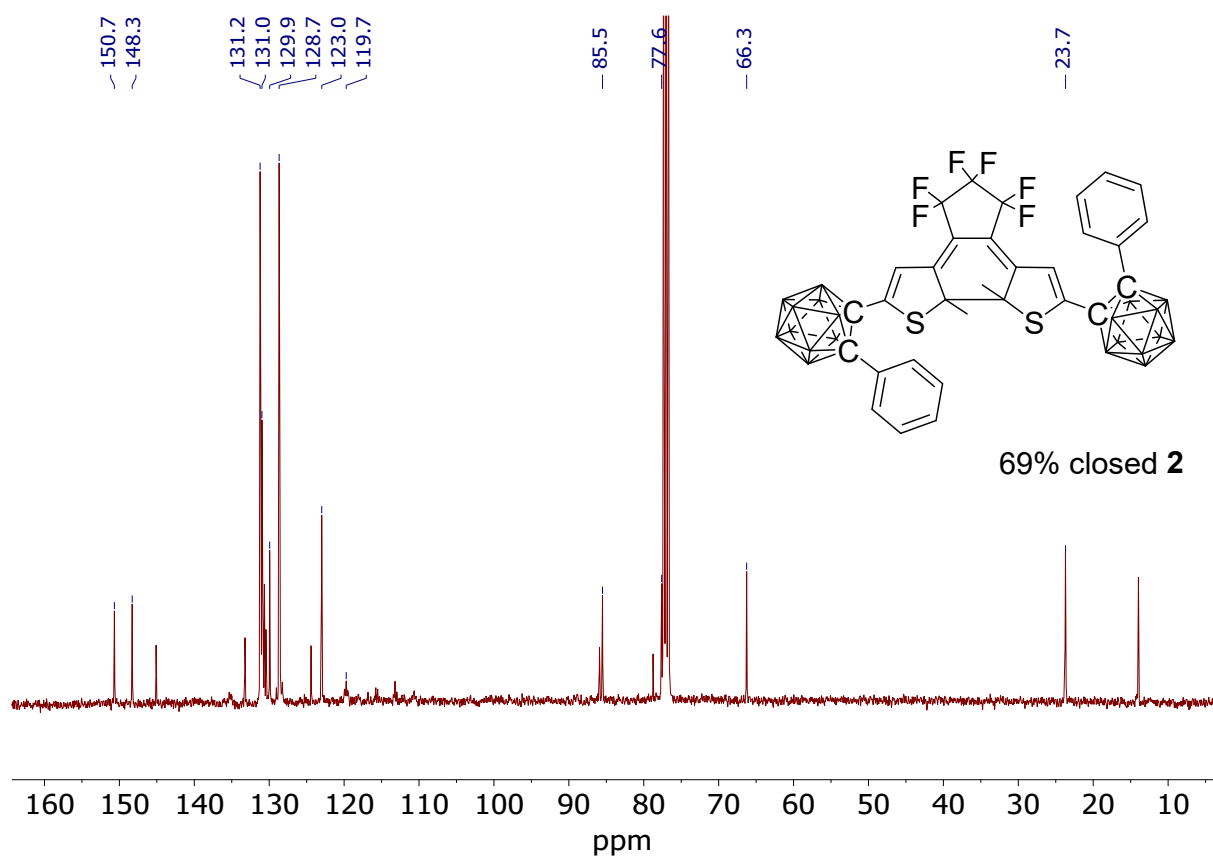


**Figure S12.**  $^{13}\text{C}\{^1\text{H}\}$  NMR spectrum for closed **2**.

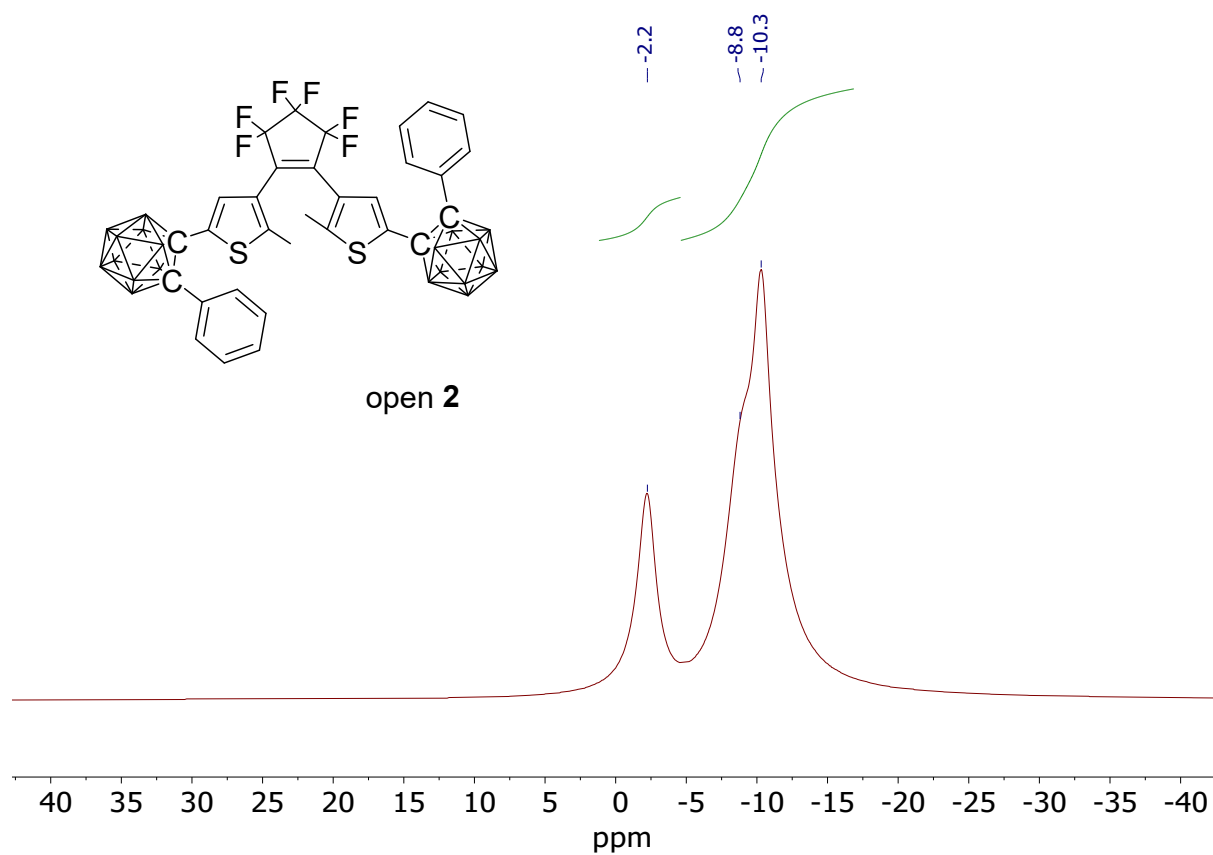


**Figure S13.**  $^{11}\text{B}\{^1\text{H}\}$  NMR spectrum for **open 2**.

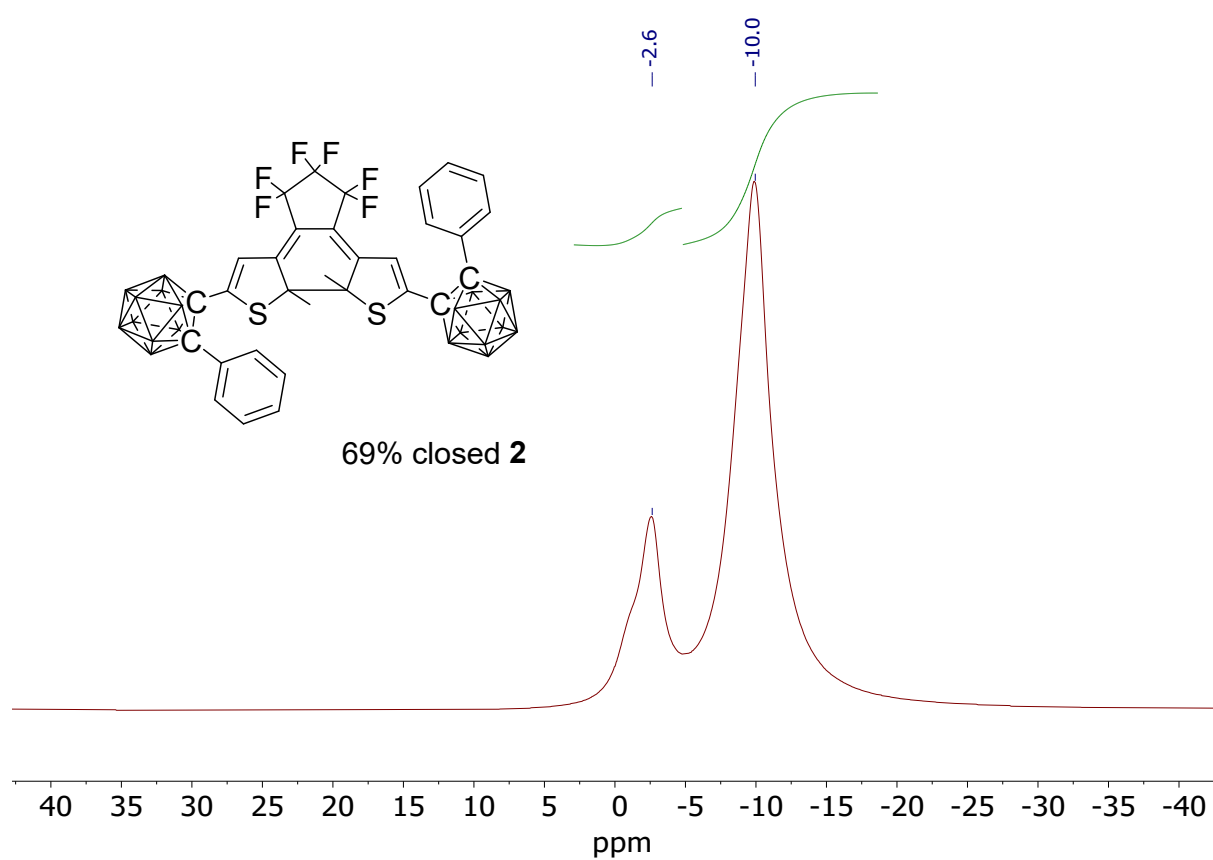


**Figure S14.**  $^{11}\text{B}\{^1\text{H}\}$  NMR spectrum for **closed 2**.

## Mass Spectra for 1 and 2

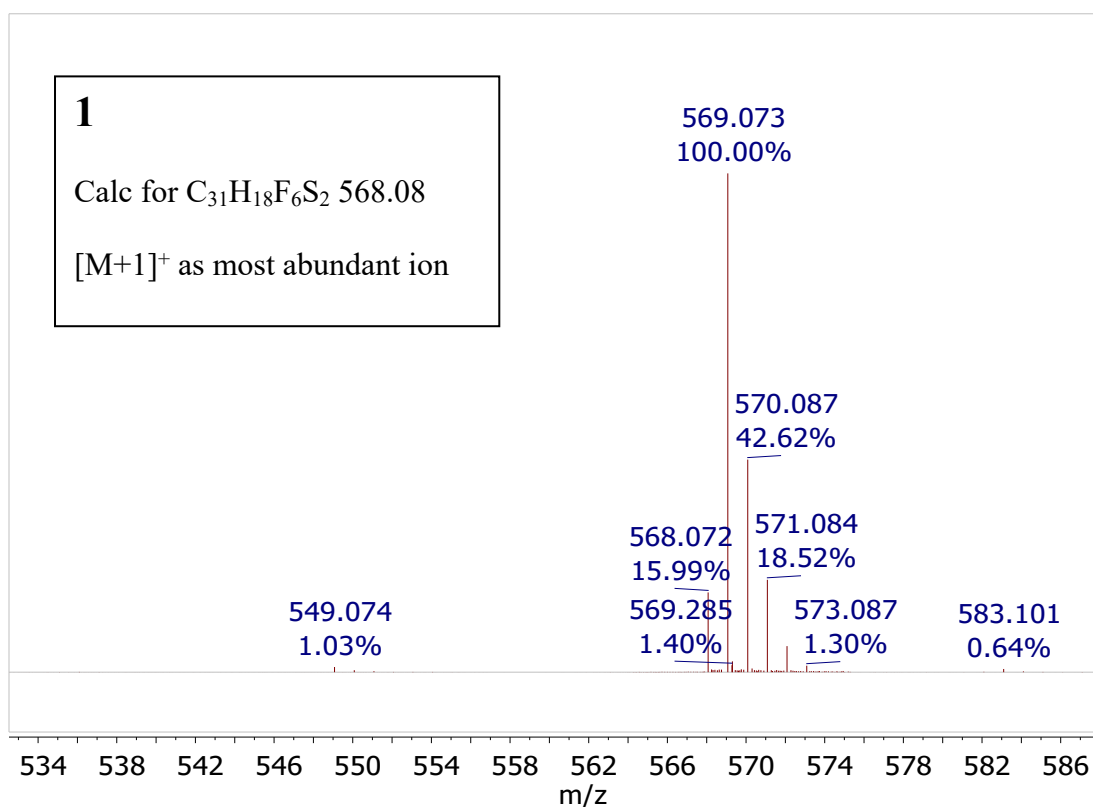


**Figure S15.** ASAP mass spectrum of **1**.

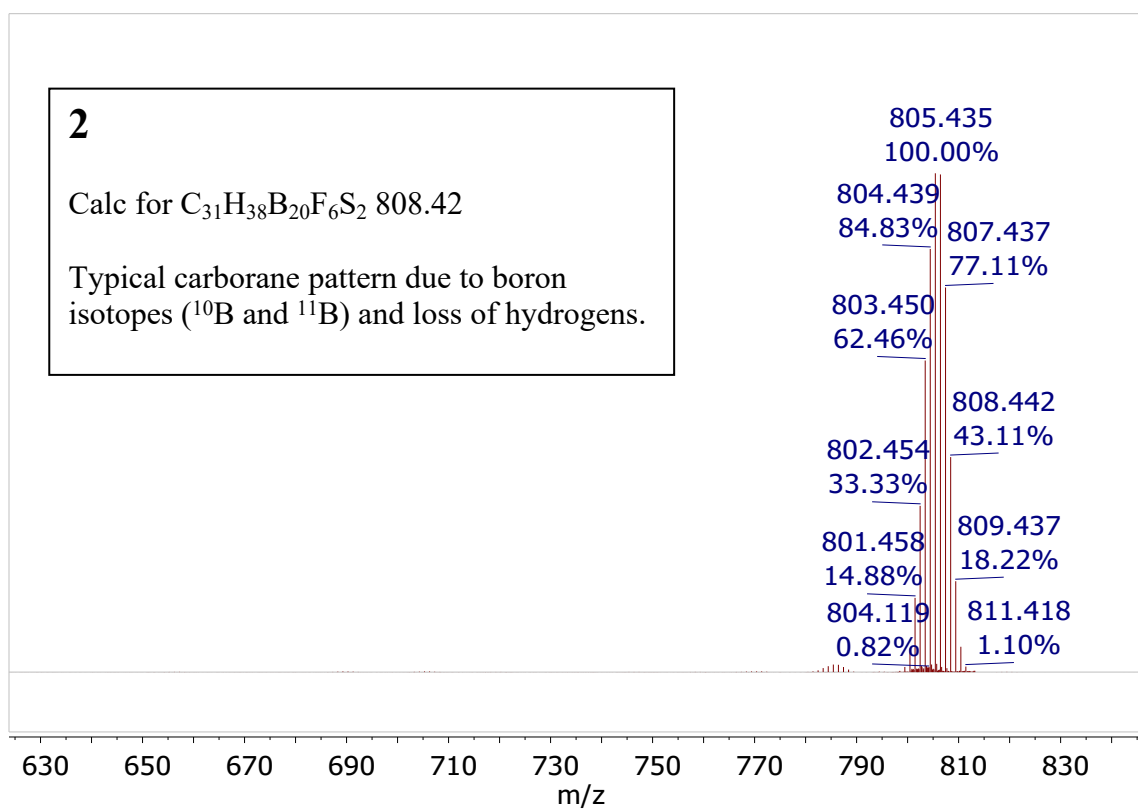


**Figure S16.** ASAP mass spectrum of **2**.

## IR Spectra for **1** and **2**

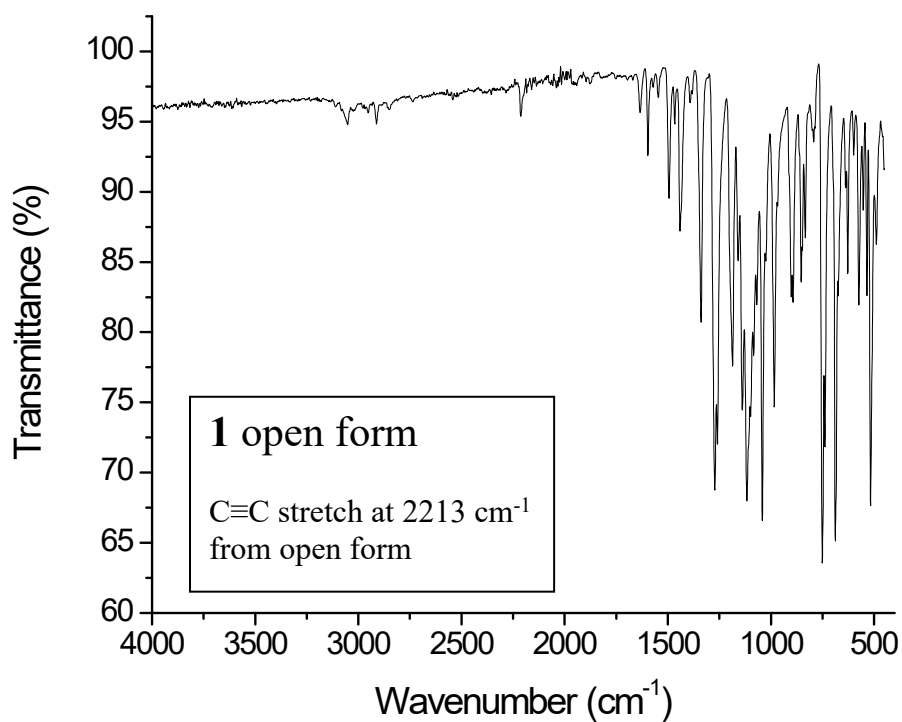


**Figure S17.** Solid state infrared (IR) spectrum of **1**.

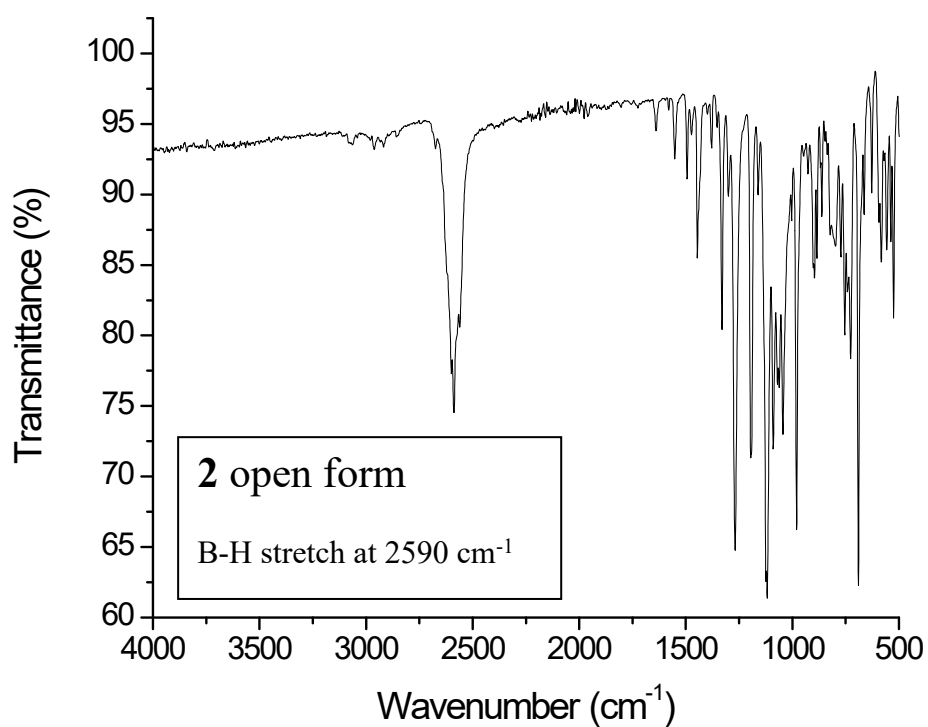


**Figure S18.** Solid state IR spectrum of **2**.

Photophysical measurements of powdered form of **2**

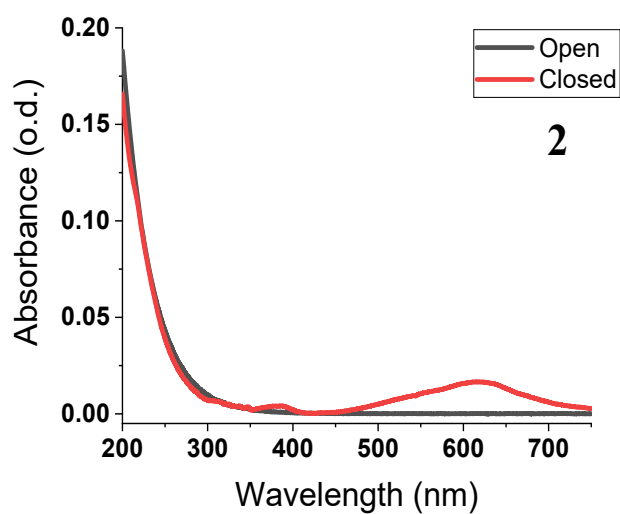


**Figure S19.** Absorption spectra for powdered form of **2**.

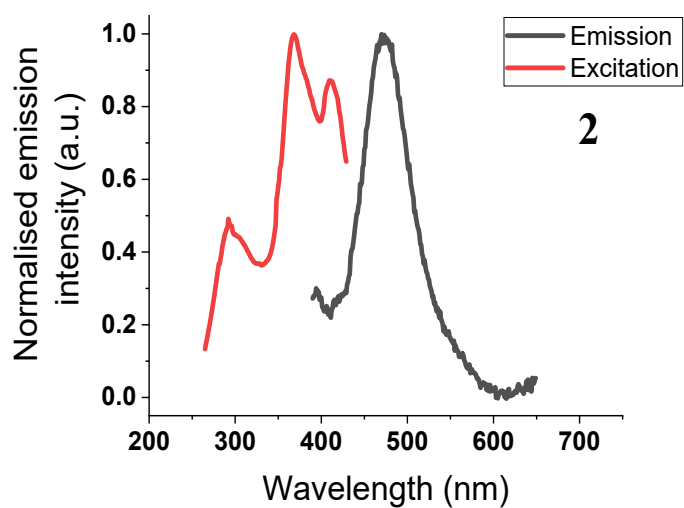


**Figure S20.** Solid state excitation and emission spectra for powdered form of **2**.

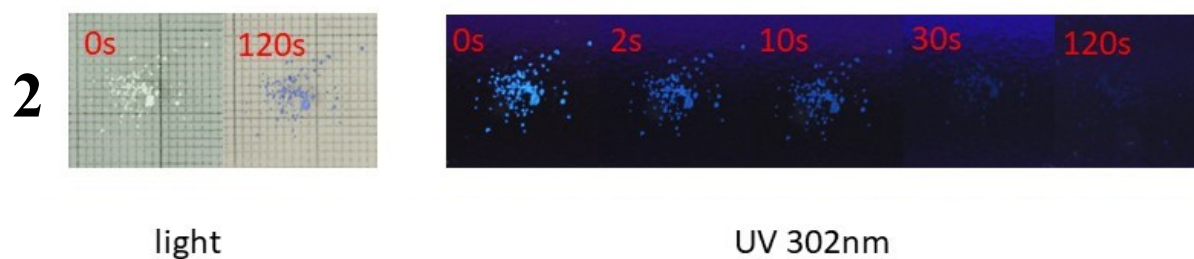


**Figure S21.** Photographs of the effect of 302 nm UV irradiation on powdered form of **2** over time.

## Photophysical measurements of PMMA film of **2**

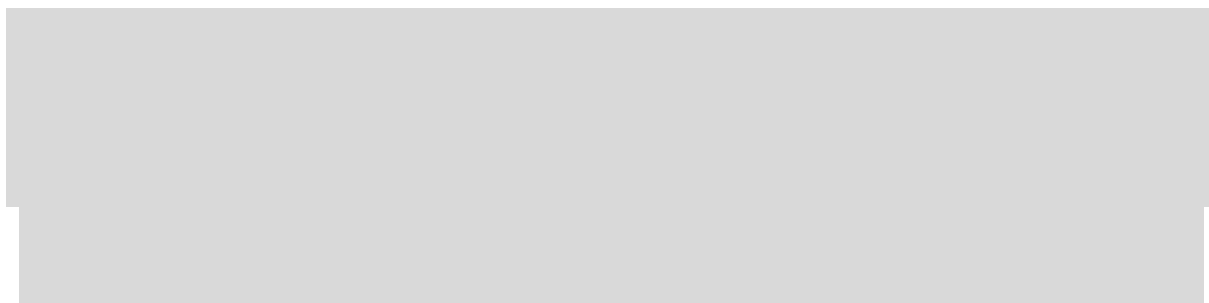


**Figure S22.** Photographs of the effect of 302 nm UV irradiation on PMMA film of **2** over time.

## Photophysical measurements of H<sub>2</sub>O: THF mixtures of **2**

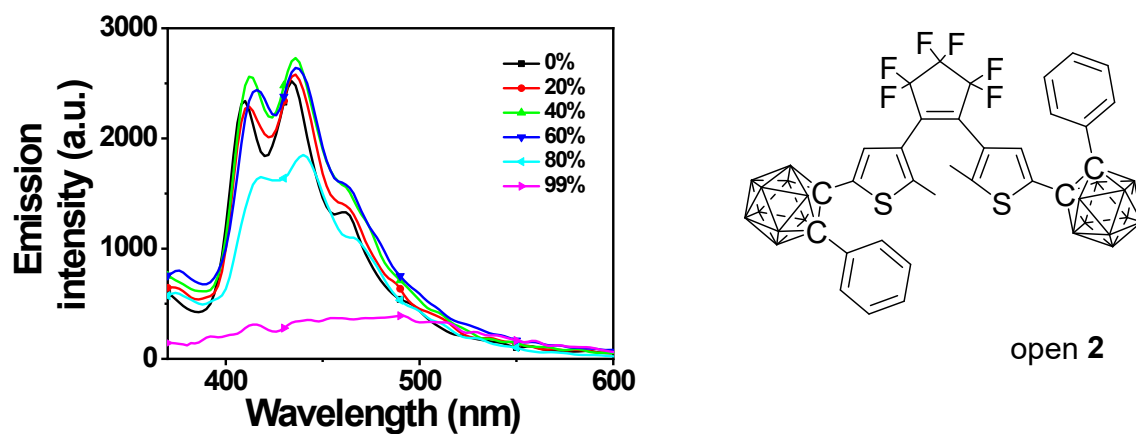


**Figure S23.** Emission spectra of **2** in water:THF mixtures with percentages given for water.



0% 99%  
Before UV  
irradiation



0% 99%  
After 60s UV  
irradiation

**Figure S24.** Photographs of **2** in THF and 99:1 water:THF under 302 nm UV light.

## Photophysical measurements of **1** in solvents

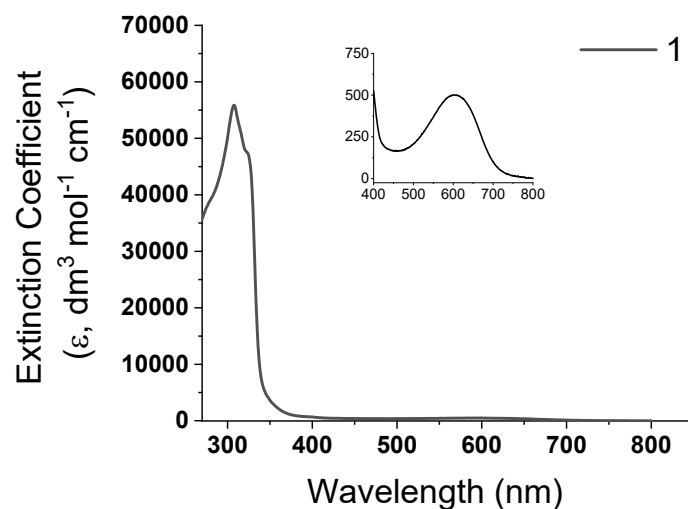


**Figure S25.** Absorption spectra of **1** ( $1 \times 10^{-6}$  M in THF) in its natural state. Inset is spectrum showing the closed form.

**Table S1.** Absorption and emission data for **1** in THF. No emissions observed for **1**.

	Absorption maxima [nm]	Emission maxima [nm]
<b>1o</b>	306, 321	-
<b>1c</b>	339, 389, 606	-

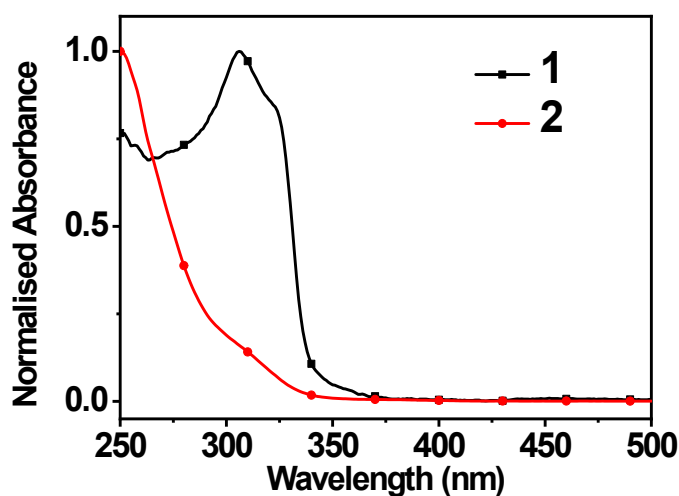


**Figure S26.** Comparison of the normalised absorption spectra of open forms of **1** and **2**. Solvent = THF, concentration =  $2 \times 10^{-5}$  M. The lower energy band in **1** is due to a  $\pi(\text{ethyne}) \rightarrow \pi^*(\text{ethyne})$  transition confirmed by time dependent-density functional theory (TD-DFT) computations.

## Photophysical measurements of **2** in solvents

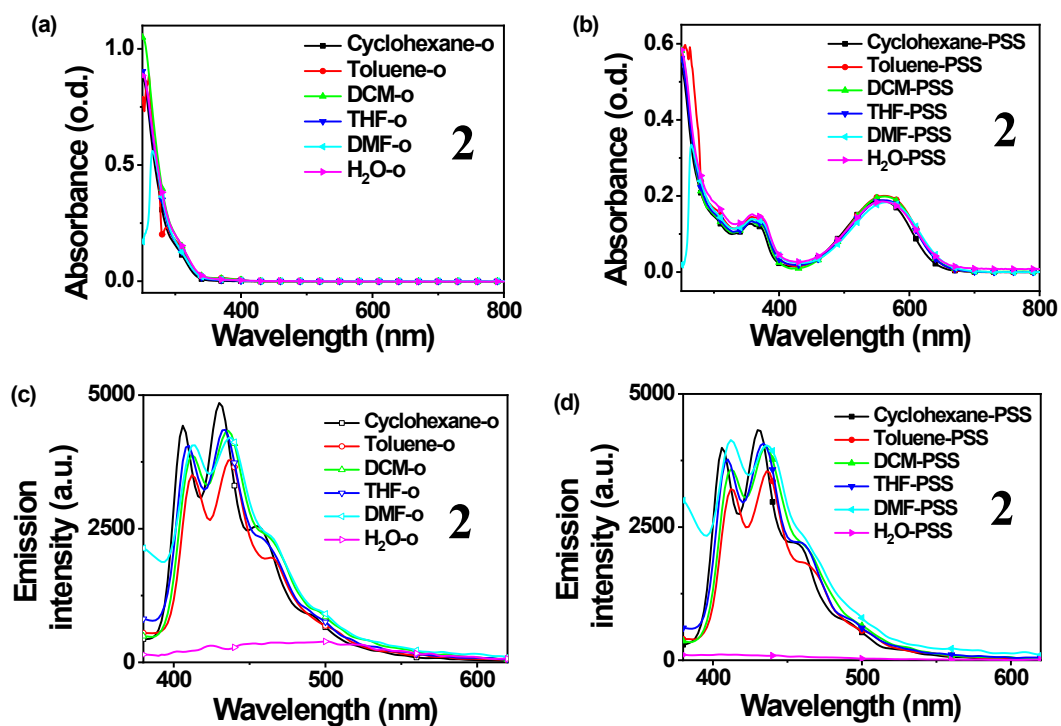


**Figure S27.** Absorption spectra and fluorescence spectra of open state (o) and photostationary state (PSS) in different polarity solvents for **2**. The H<sub>2</sub>O label is 99:1 H<sub>2</sub>O:THF solvent mixture where solid particulates of **2** are expected.

**Table S2.** Absorption maxima in wavelengths (nm) for **2**. No maxima were observed for **2o** (open form of **2**) at wavelengths longer than 250 nm. The closed form **2c** has a low energy band around 560 nm arising from  $\pi(\text{DTE}) \rightarrow \pi^*(\text{DTE})$  local transitions confirmed by TD-DFT computations.

	Cyclohexane	Toluene	Dichloromethane	Tetrahydrofuran	Dimethylformamide	99:1 water:THF	PMMA films	Powder solids
<b>2c</b>	356, 368, 556	358, 371, 562	357, 368, 562	358, 369, 562	359, 370, 567	359, 370, 559	353, 370, 560	382, 618

**Table S3.** Emission data in nm for **2** showing the different emissions observed; local emission (LE) and solid state (SS) emissions.

		Cyclohexane	Toluene	Dichloromethane	Tetrahydrofuran	Dimethylformamide	99:1 water:THF	PMMA films	Powder solids
<b>2o</b>	LE	406, 430, 455	412, 437, 465	412, 436, 461	409, 433, 455	413, 436, 460			
	SS						497	480	474
<b>2c</b>	LE	407, 431, 454	413, 437, 461	412, 436, 464	410, 433, 457	412, 436, 459	-	-	-

## Lifetime measurements for **2**

**Table S4.** Lifetimes for open form of **2**. No emission was found for **1**.

		Emission Type <sup>a)</sup>	Emission maxima [nm]	$\tau_{av}$ [ns]	Lifetime <sup>b)</sup>	
					$\tau_1$ [ns]	$\tau_2$ [ns]
<b>2</b>	THF	LE		0.76	0.42	1.64
	99:1 water:THF	SS		1.19	0.70	4.48
	Powder	SS		1.02	0.91	11.80

<sup>a)</sup> LE = Local emission, SS = Solid state emission.

<sup>b)</sup> Lifetime values of  $\tau_1$  and  $\tau_2$  determined from biexponential curve fittings.

## Photoisomerisation measurements

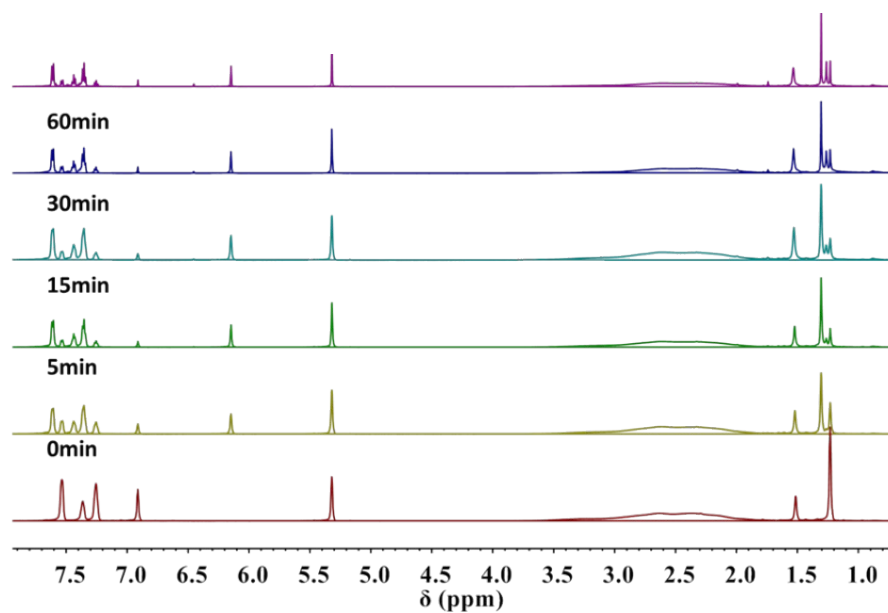


**Figure S28.** The <sup>1</sup>H NMR spectra for **2** during 302 nm UV-light irradiation and used for  $\alpha_{\text{pss}}$  values. Solvent = CD<sub>2</sub>Cl<sub>2</sub>.

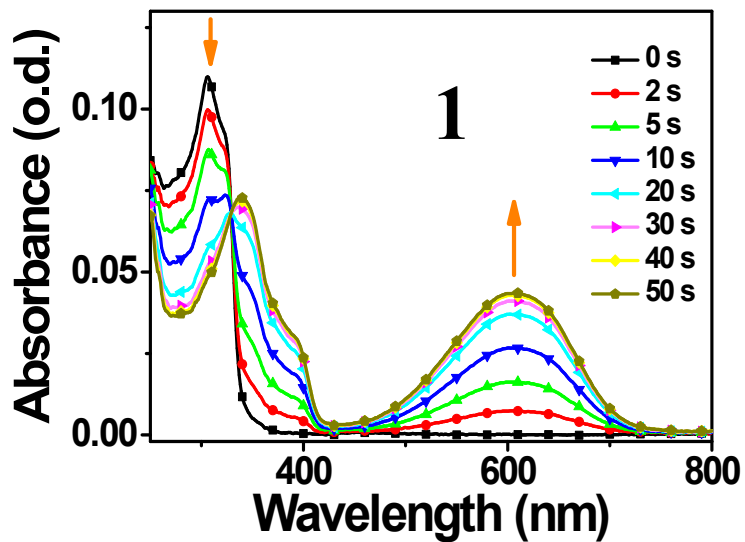


**Figure S29.** The absorption spectra of **1** upon UV-light irradiation, showing the transition from open form to closed form (photocyclisation), concentration =  $2 \times 10^{-6}$  M in THF.

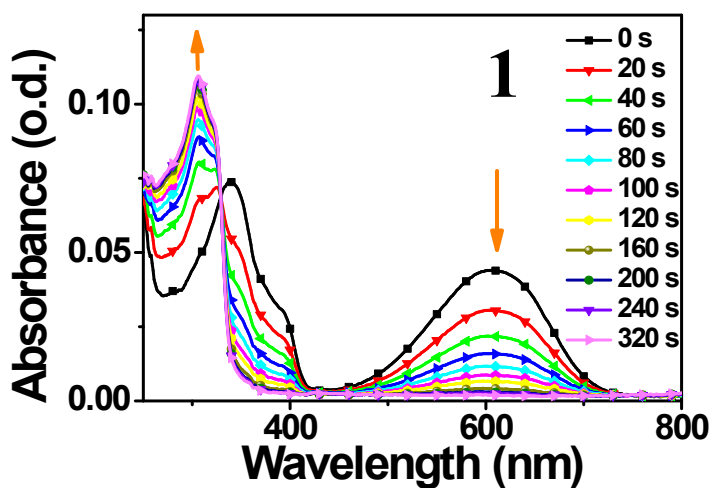


**Figure S30.** The absorption spectra of **1** at the photo-stationary state (PSS) upon visible-light irradiation showing the reverse transition from closed form to open form, concentration =  $2 \times 10^{-6}$  M in THF and the irradiation wavelength = 621 nm ( $7.68 \text{ mW/cm}^2$ ).

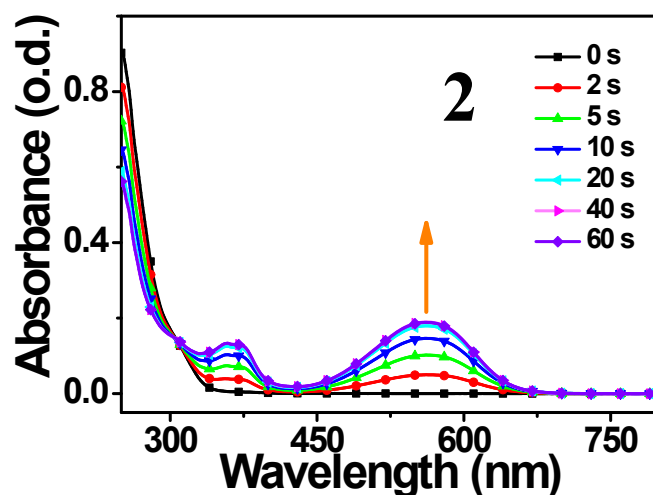


**Figure S31.** The absorption spectra of **2** upon UV-light irradiation showing the transition from open form to closed form (photocyclisation), concentration is  $2 \times 10^{-6}$  M in THF and the irradiation wavelength is 302 nm ( $0.47 \text{ mW/cm}^2$ ).

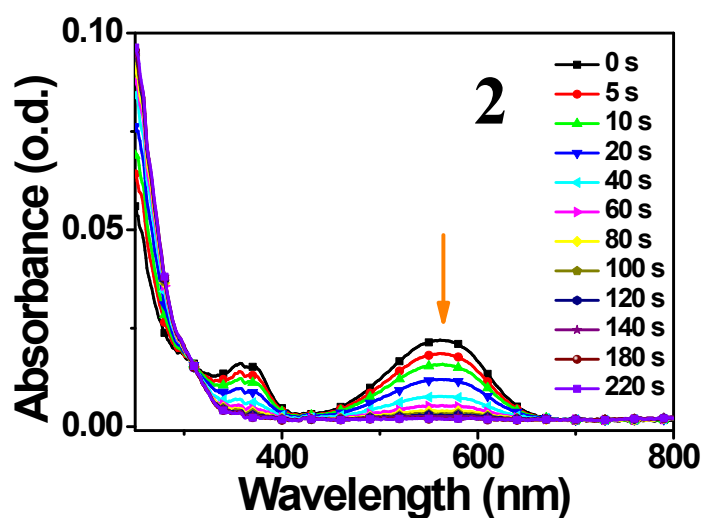


**Figure S32.** The absorption spectra of **2** at the photo-stationary state (PSS) upon visible-light irradiation showing the reverse transition from closed form to open form, concentration is  $2 \times 10^{-6}$  M in THF and the irradiation wavelength is 621 nm ( $7.68 \text{ mW/cm}^2$ ).

## Cyclic voltammetry

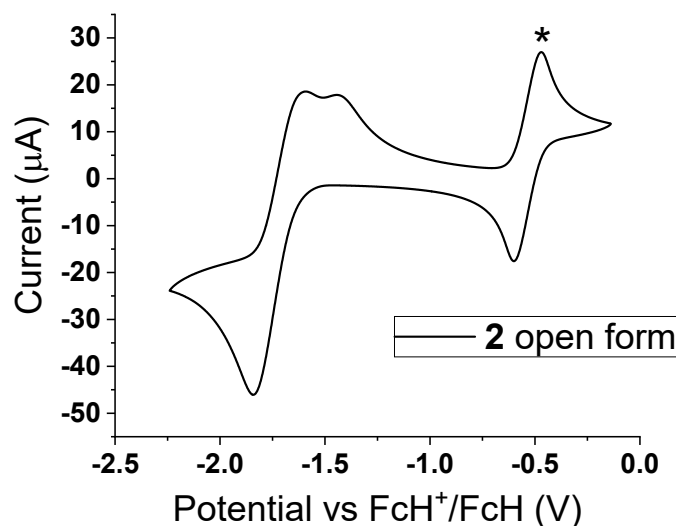


**Figure S33.** CV trace for open **2** in 0.1 M  $n\text{Bu}_4\text{NPF}_6$  in DCM. The decamethylferrocenium /decamethylferrocene  $[(\text{C}_5\text{Me}_5)_2\text{Fe}^+/(\text{C}_5\text{Me}_5)_2\text{Fe}; (\text{Cp}^*\text{Fe}^+/\text{Cp}^*\text{Fe})]$  internal reference couple is shown with an asterisk at  $E_{1/2} = -0.53$  V. The potential is referenced against the ferrocenium/ferrocene reference couple  $(\text{C}_5\text{H}_5)_2\text{Fe}^+/(\text{C}_5\text{H}_5)_2\text{Fe}$  ( $\text{Cp}_2\text{Fe}^+/\text{Cp}_2\text{Fe}$ ) at  $E_{1/2} = 0.00$  V (abbreviated as  $\text{FcH}^+/\text{FcH}$  at 0.00 V). Fc is ferrocenyl  $(\text{C}_5\text{H}_5)\text{Fe}(\text{C}_5\text{H}_4)$ .

**Table S5.** Reduction potentials for open form of **2** with 0.1 M  $n\text{Bu}_4\text{NPF}_6$  in DCM as electrolyte solution. No waves within the solvent window were observed for open form of **1**.

	E(Red1) cathodic <sup>a)</sup> [V]	E(Red1) anodic <sup>b)</sup> [V]	$E_{1/2}$ (Red1) [V]	p-p <sup>c)</sup> Red1 [mV]	E(Red2) cathodic <sup>d)</sup> [V]	E(Red2) anodic <sup>e)</sup> [V]	$E_{1/2}$ (Red2) [V]	p-p <sup>c)</sup> Red2 [mV]	$E_{1/2}$ (Red1)- $E_{1/2}$ (Red2) [mV]
<b>2o</b>	-1.84 <sup>f)</sup>	-1.44	-1.64	400	-1.84 <sup>f)</sup>	-1.59	-1.72	250	150

<sup>a)</sup> cathodic wave of first one-electron reduction at each cluster.

<sup>b)</sup> anodic wave of first one-electron reduction at each cluster.

<sup>c)</sup> peak separation between anodic and cathodic peaks.

<sup>d)</sup> cathodic wave of second one-electron reduction at each cluster.

<sup>e)</sup> anodic wave of second one-electron reduction at each cluster.

<sup>f)</sup> one two-electron reduction cathodic wave at each cluster.

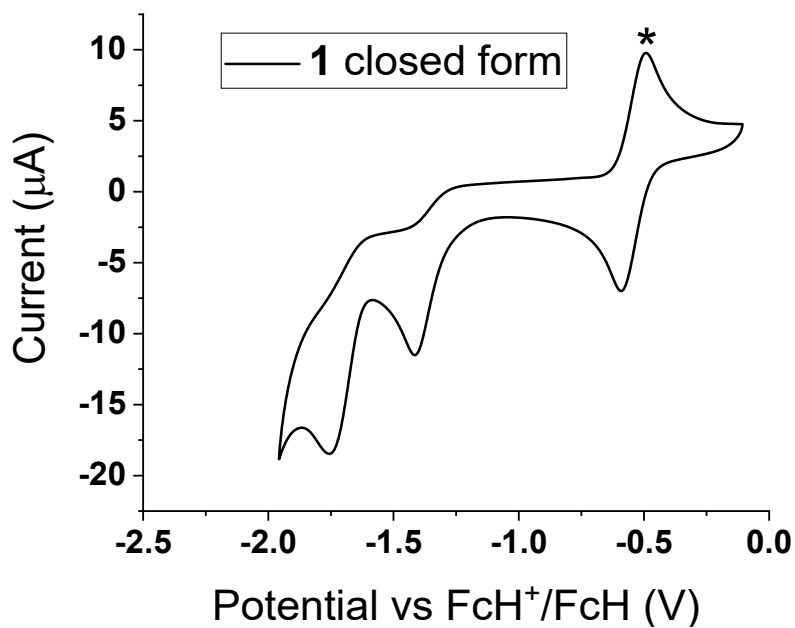


**Figure S34.** CV trace for closed form of **1**. The decamethylferrocenium/decamethylferrocene internal reference couple ( $\text{Cp}^*\text{Fe}^+/\text{Cp}^*\text{Fe}$ ) is shown with an asterisk.

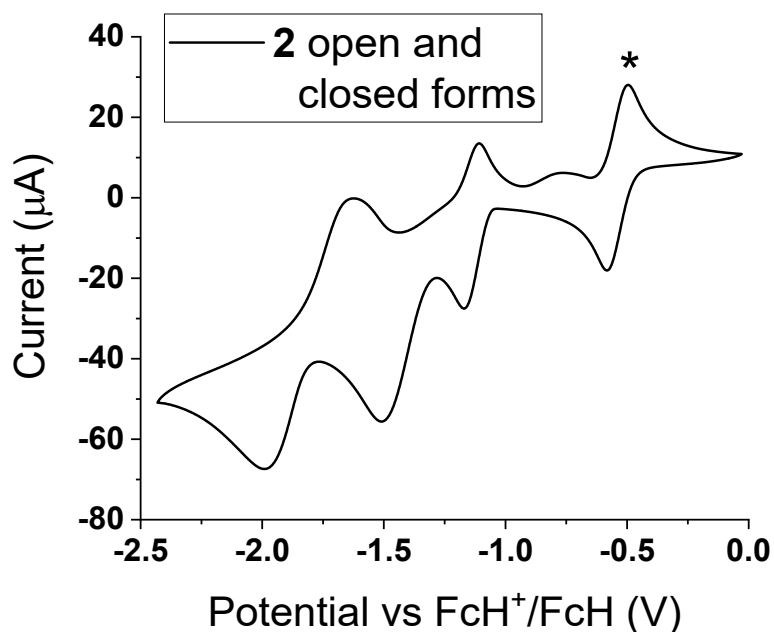


**Figure S35.** CV trace for a mixture of open and closed forms of **2**. The decamethylferrocenium/decamethylferrocene internal reference couple ( $\text{Cp}^*\text{Fe}^+/\text{Cp}^*\text{Fe}$ ) is shown with an asterisk.

**Table S6.** CV data for closed forms of **1** and mixture of open and closed forms of **2**. All waves are irreversible.

	E(Red1)	E(Red2)	E(Ox1)
	cathodic <sup>a)</sup>	cathodic	anodic
	[V]	[V]	[V]
<b>1c</b>	-1.41	-1.74	0.76 <sup>b)</sup>
<b>2c</b>	-1.16	-1.50	1.11 <sup>b)</sup>

<sup>a)</sup> cathodic wave of first two-electron reduction at the closed dithienylethene (DTE) unit.

<sup>b)</sup> anodic wave of first two-electron oxidation at the closed dithienylethene (DTE) unit.

## Single-crystal X-ray crystallography

**Table S7.** Crystal data and structure refinement parameters.

Compound	<b>1</b>	<b>2</b>
Empirical formula	C <sub>31</sub> H <sub>18</sub> F <sub>6</sub> S <sub>2</sub>	C <sub>31</sub> H <sub>38</sub> B <sub>20</sub> F <sub>6</sub> S <sub>2</sub> (x 1.5 C <sub>7</sub> H <sub>8</sub> )
Formula weight	568.57	943.14
Temperature/K	120.0	120.0
Crystal system	triclinic	monoclinic
Space group	P-1	P2 <sub>1</sub> /c
a/Å	10.7814(2)	10.9309(2)
b/Å	14.0893(3)	25.9004(5)
c/Å	18.4393(4)	17.5286(3)
α/°	100.450(2)	90.00
β/°	101.1462(19)	102.900(3)
γ/°	101.4357(19)	90.00
Volume/Å <sup>3</sup>	2622.32(10)	4837.36(15)
Z	4	4
ρ <sub>calc</sub> /cm <sup>3</sup>	1.440	1.295
μ/mm <sup>-1</sup>	0.266	0.167
F(000)	1160.0	1940.0
Radiation, λ (Å)	MoKα, 0.71073	MoKα, 0.71073
Reflections collected	51544	87745
Independent refl., R <sub>int</sub>	13949, 0.0428	11671, 0.0627
Data/restraints/parameters	13949/55/698	11671/66/618
Goodness-of-fit on F <sup>2</sup>	1.043	1.017
Final R <sub>1</sub> [I ≥ 2σ (I)]	0.0612	0.0633
Final wR <sub>2</sub> [all data]	0.1554	0.1613
Max diff. peak/hole, e Å <sup>-3</sup>	1.41/-0.81	0.94/-0.78

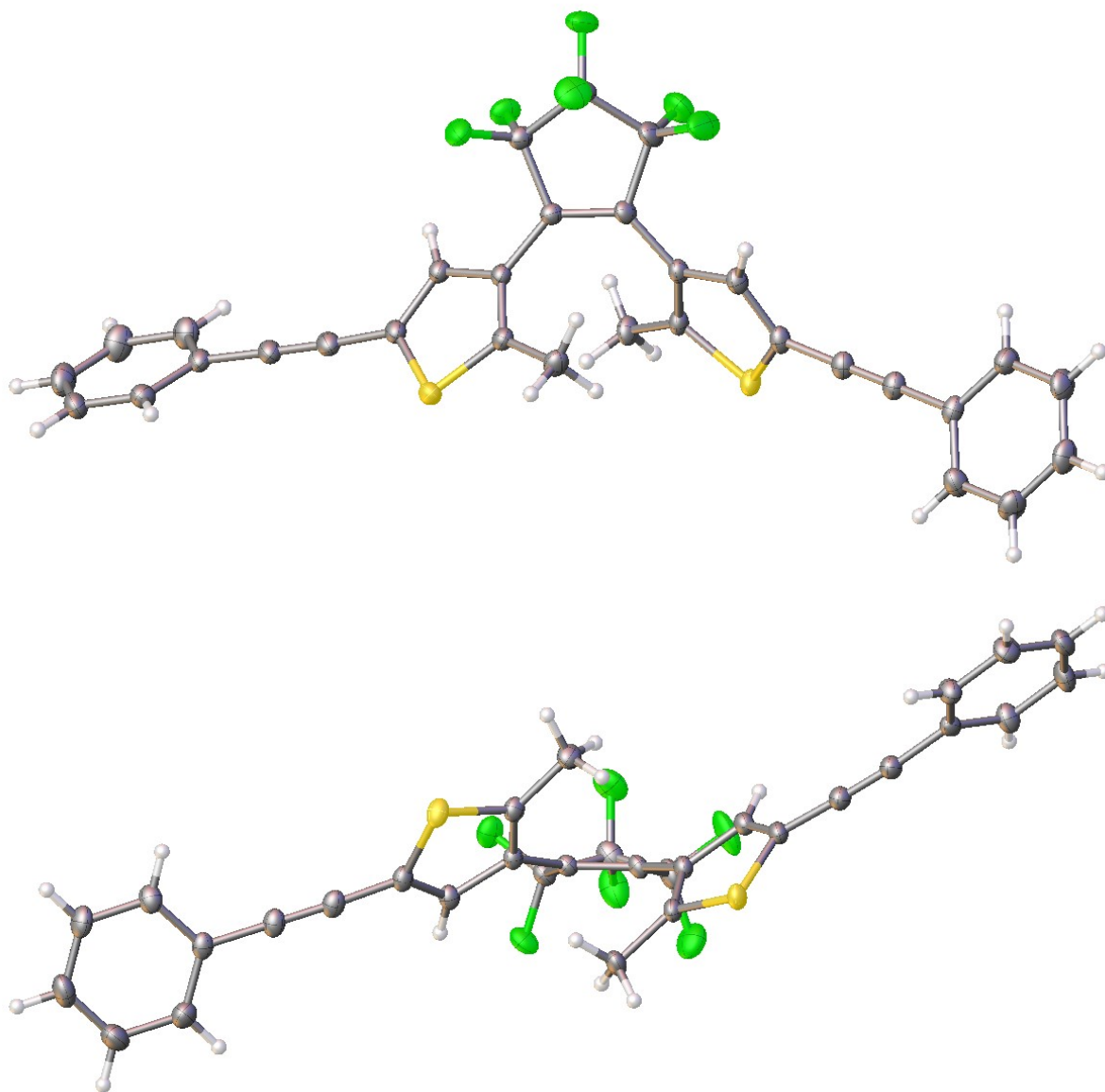


**Figure S37.** Two views of the experimental (X-ray) molecular geometry of one independent molecule in crystal of **1**.

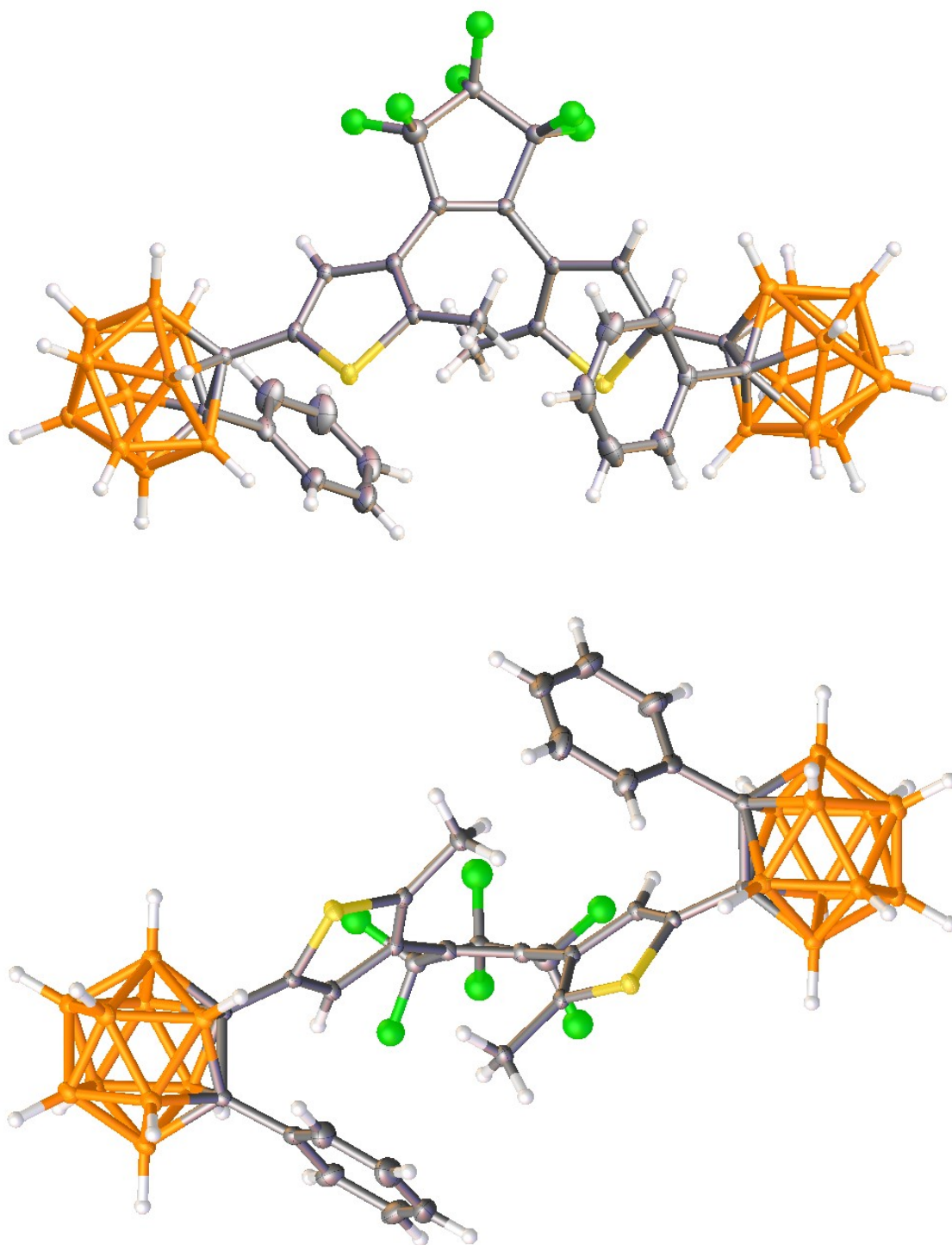


**Figure S38.** Two views of the experimental (X-ray) molecular geometry in crystal of **2**.

## Optimised Geometries

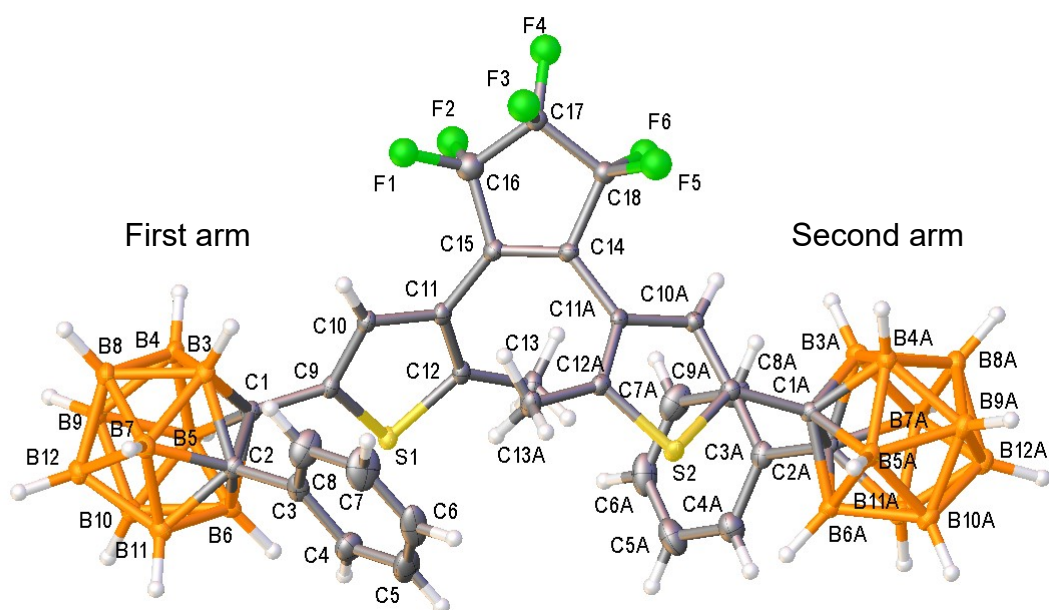


**Figure S39.** Atom numbering scheme used for comparison between experimental (X-ray) and optimised (B3LYP/6-31G(d)/GD3BJ) geometries in **1** and **2**.

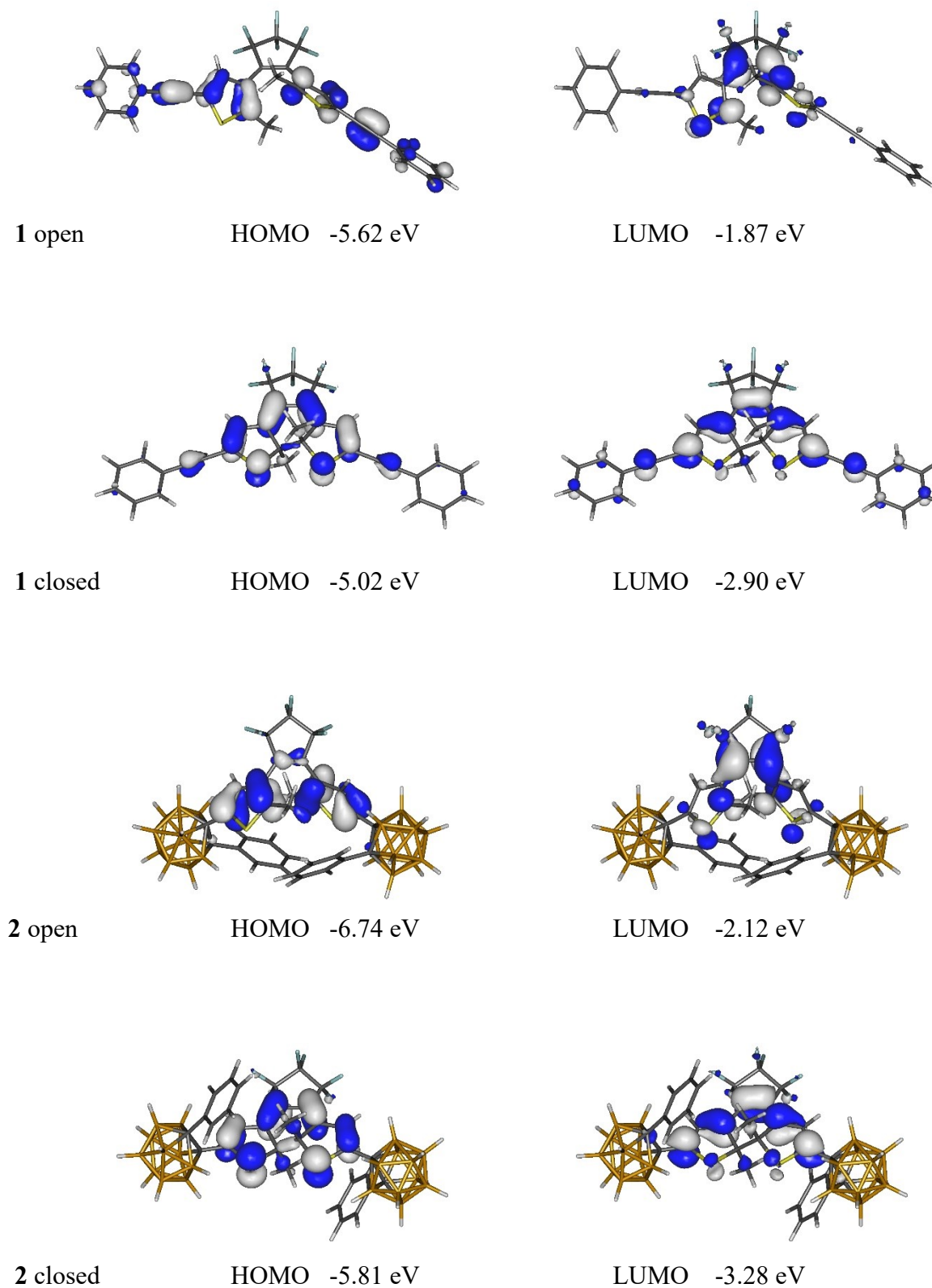
**Table S8.** Comparison of selected bond lengths in angstroms (Å) between experimental (X-ray) and optimised (hybrid DFT) geometries for **1**. One of two independent molecules of **1** in crystal is measured. The second independent molecule contains a disordered perfluorocyclopentane ring.

	X-ray	X-ray	Averaged	Calculated	Difference
	First arm	Second arm			
C1-C2	1.198	1.195	1.197	1.217	0.020
C1-C9	1.419	1.425	1.422	1.403	0.019
C2-C3	1.432	1.440	1.436	1.421	0.015
C9-S1	1.733	1.734	1.734	1.762	0.028
C12-S1	1.715	1.723	1.719	1.738	0.019
C9-C10	1.368	1.365	1.367	1.376	0.009
C10-C11	1.429	1.432	1.431	1.431	0.000
C11-C12	1.382	1.381	1.382	1.385	0.003
C11-C15	1.463	1.465	1.464	1.464	0.000
C15-C14	1.356	1.356	1.356	1.356	0.000
C15-C16	1.505	1.510	1.508	1.510	0.002
C16-C17	1.536	1.534	1.535	1.549	0.014

**Table S9.** Comparison of selected bond lengths in angstroms (Å) between experimental and optimised geometries for **2**. A disordered perfluorocyclopentane ring is present in the crystal of **2** (disorder values in italics).

	X-ray First arm	X-ray Second arm	Averaged	Calculated	Difference
C1-C2	1.728	1.727	1.728	1.742	0.014
C1-C9	1.479	1.477	1.478	1.474	0.004
C2-C3	1.502	1.504	1.503	1.502	0.001
C9-S1	1.723	1.726	1.725	1.750	0.025
C12-S1	1.716	1.718	1.717	1.733	0.016
C9-C10	1.359	1.358	1.359	1.369	0.010
C10-C11	1.424	1.425	1.425	1.431	0.006
C11-C12	1.379	1.374	1.377	1.382	0.005
C11-C15	1.463	1.467	1.465	1.463	0.002
C15-C14	1.347	1.347	1.347	1.351	0.004
C15-C16	<i>1.505</i>	<i>1.518</i>	<i>1.512</i>	1.505	<i>0.007</i>
C16-C17	<i>1.520</i>	<i>1.507</i>	<i>1.514</i>	1.553	<i>0.039</i>

**Figure S40.** Frontier orbitals in open and closed forms of **1** and **2**. Contours are drawn at  $\pm 0.04$  (e/bohr<sup>3</sup>)<sup>1/2</sup>.



## Simulated absorption spectra

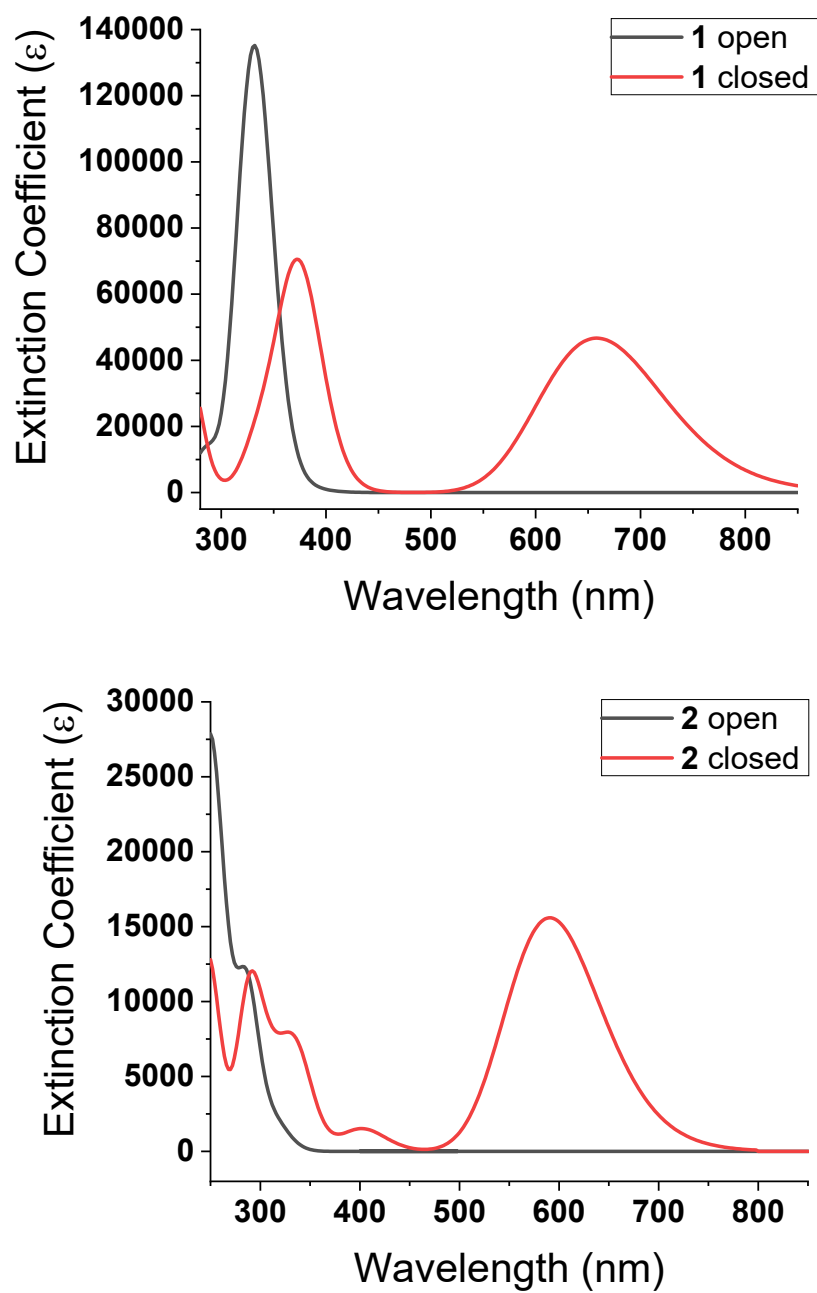


**Figure S41.** Simulated absorption spectra of open and closed forms of **1** and **2** from 80 singlet states by TD-DFT computations. The gaussian bands were generated at the half height half width (hhhw) of 0.2 eV and the extinction coefficients were obtained by oscillator strengths times 240000. The spectra are in broad agreement with experimental absorption spectra.

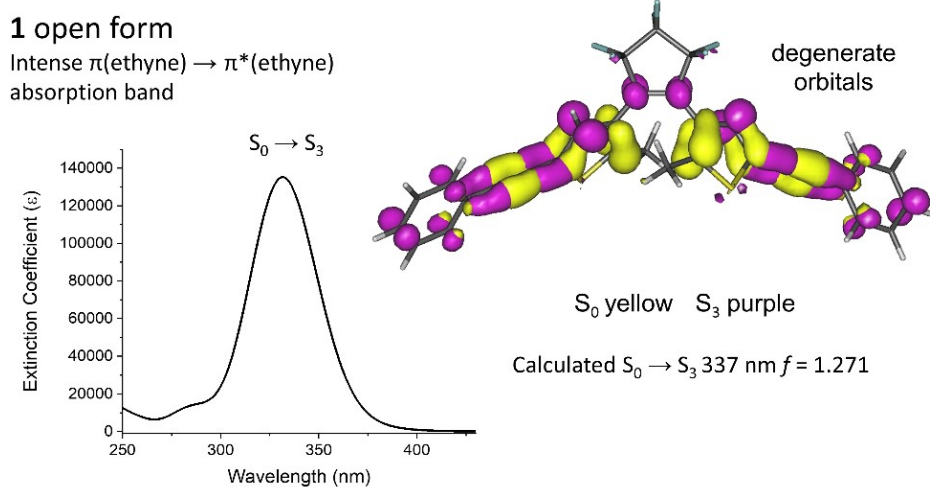


**Figure S42.** Assignment of the dominant low energy absorption band for the open form of **1** from TD-DFT computations with the natural transition orbitals involved in the  $\pi(\text{ethynyl}) \rightarrow \pi^*(\text{ethynyl})$  transition.

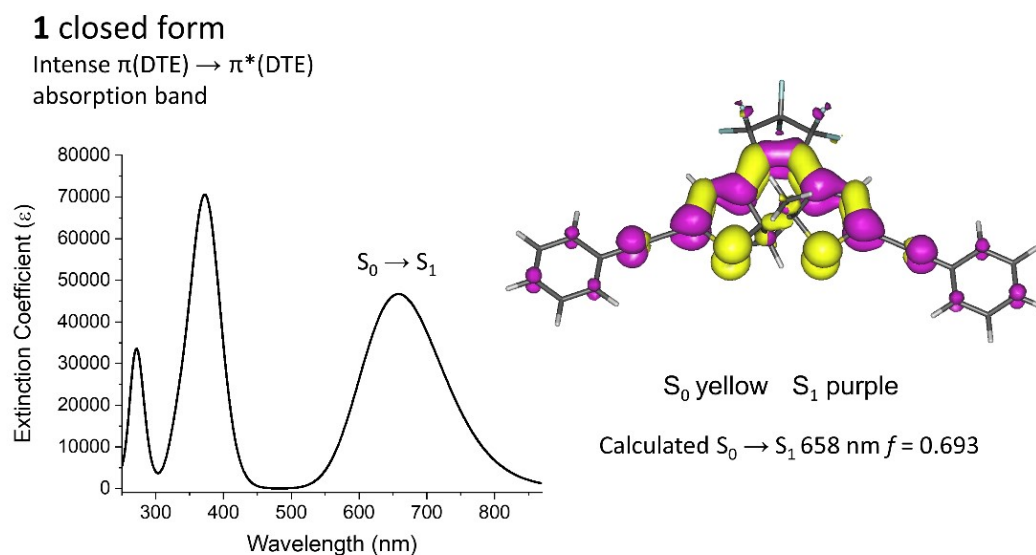


**Figure S43.** Assignment of the dominant low energy absorption band for the closed form of **1** from TD-DFT computations with the natural transition orbitals involved in the  $\pi(\text{DTE}) \rightarrow \pi^*(\text{DTE})$  transition.

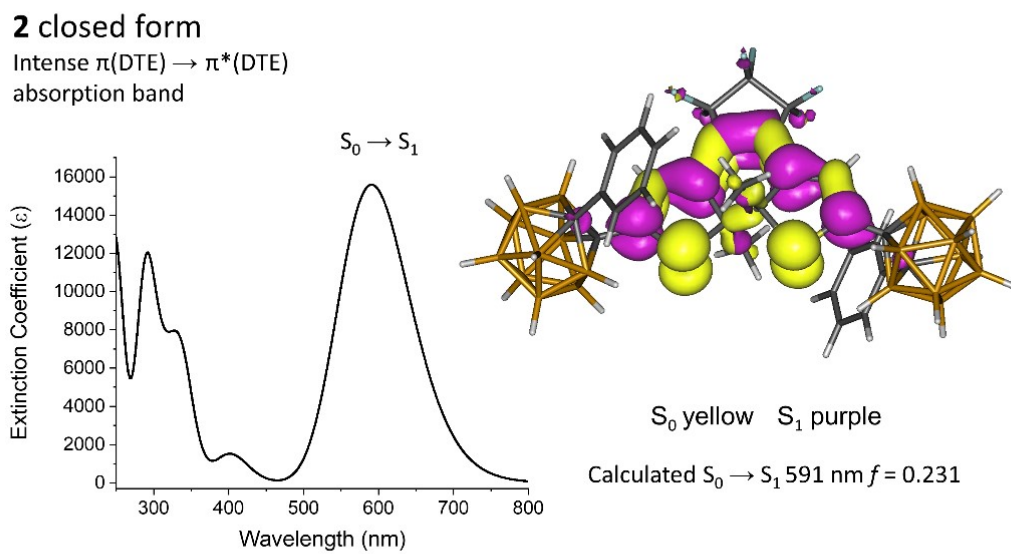


**Figure S44.** Assignment of the dominant low energy absorption band for the closed form of **2** from TD-DFT computations with the natural transition orbitals involved in the  $\pi(\text{DTE}) \rightarrow \pi^*(\text{DTE})$  transition.

## References

1. T. Saika, M. Irie, T. Shimidzu, Thiophene Oligomers with a Photoswitch *J. Chem. Soc., Chem. Commun.* **1994**, 2123-2124.
2. F. Gillanders, L. Giordano, S. A. Diaz, T. M. Jovin, E. A. Jares-Erijman, Photoswitchable fluorescent diheteroarylethenes: substituent effects on photochromic and solvatochromic properties. *Photochem. Photobiol. Sci.* **2014**, 13, 603-612.
3. L. Giordano, T. M. Jovin, M. Irie, E. A. Jares-Erijman, Diheteroarylethenes as thermally stable photoswitchable acceptors in photochromic fluorescence resonance energy transfer (pcFRET). *J. Am. Chem. Soc.* **2002**, 124, 7481-7489.
4. C. Li, H. Yan, L. X. Zhao, G. F. Zhang, Z. Hu, Z. L. Huang, M. Q. Zhu, A trident dithienylethene-perylenemonoimide dyad with super fluorescence switching speed and ratio. *Nat. Commun.* **2014**, 5, 5709.
5. O. V. Dolomanov, L. J. Bourhis, R. J. Gildea, J. A. K. Howard and H. Puschmann, OLEX2: A Complete Structure Solution, Refinement and Analysis Program. *J. Appl. Crystallogr.* 2009, **42**, 339-341.
6. G.M. Sheldrick, A short history of SHELX *Acta Cryst.* **2008**, A64, 112-122.
7. M. J. Frisch, G. W. Trucks, H. B. Schlegel, G. E. Scuseria, M. A. Robb, J. R. Cheeseman, G. Scalmani, V. Barone, G. A. Petersson, H. Nakatsuji, X. Li, M. Caricato, A. V. Marenich, J. Bloino, B. G. Janesko, R. Gomperts, B. Mennucci, H. P. Hratchian, J. V. Ortiz, A. F. Izmaylov, J. L. Sonnenberg, D. Williams-Young, F. Ding, F. Lipparini, F. Egidi, J. Goings, B. Peng, A. Petrone, T. Henderson, D. Ranasinghe, V. G. Zakrzewski, J. Gao, N. Rega, G. Zheng, W. Liang, M. Hada, M. Ehara, K. Toyota, R. Fukuda, J. Hasegawa, M. Ishida, T. Nakajima, Y. Honda, O. Kitao, H. Nakai, T. Vreven, K. Throssell, J. A. Montgomery, Jr., J. E. Peralta, F. Ogliaro, M. J. Bearpark, J. J. Heyd, E. N. Brothers, K. N. Kudin, V. N. Staroverov, T. A. Keith, R. Kobayashi, J. Normand, K. Raghavachari, A. P. Rendell, J. C. Burant, S. S. Iyengar, J. Tomasi, M. Cossi, J. M. Millam, M. Klene, C. Adamo, R. Cammi, J. W. Ochterski, R. L. Martin, K. Morokuma, O. Farkas, J. B. Foresman, and D. J. Fox, Gaussian 16, Revision B.01, Gaussian, Inc., Wallingford CT, 2016.
8. A. D. Becke, Density-Functional Thermochemistry. 3. The Role of Exact Exchange, *J. Chem. Phys.*, 1993, **98**, 5648-5652.
9. C. T. Lee, W. T. Yang and R. G. Parr, Development of the Colle-Salvetti Correlation-Energy Formula into a Functional of the Electron-Density, *Phys. Rev. B*, 1988, **37**, 785-789.
10. G. A. Petersson, A. Bennett, T. G. Tensfeldt, M. A. Al Laham, W. A. Shirley and J. Mantzaris, A Complete Basis Set Model Chemistry. 1. The Total Energies of Closed-Shell Atoms and Hydrides of the 1st-Row Elements, *J. Chem. Phys.*, 1988, **89**, 2193-2218.
11. G. A. Petersson and M. A. Al Laham, A Complete Basis Set Model Chemistry. 2. Open-Shell Systems and the Total Energies of the 1st-Row Atoms, *J. Chem. Phys.*, 1991, **94**, 6081-6090.
12. S. Grimme, S. Ehrlich and L. Goerigk, "Effect of the damping function in dispersion corrected density functional theory," *J. Comp. Chem.* 2011, **32**, 1456-65.

13. A. R. Allouche, Gabedit-A Graphical User Interface for Computational Chemistry Softwares *J. Comput. Chem.*, 2011, **32**, 174-182.
14. S. Fraysse, C. Coudret, J.-P. Launay, Synthesis and Properties of Dinuclear Complexes with a Photochromic Bridge: An Intervalence Electron Transfer Switching “On” and “Off”, *Eur. J. Inorg. Chem.* **2000**, 1581-1590.